Circulation Research

ORIGINAL RESEARCH

Cardiomyocyte PRL2 Promotes Cardiac Hypertrophy via Directly Dephosphorylating AMPKα2

Xue Han,* Qiaojuan Shi,* Yu Tu, Jiajia Zhang, Mengyang Wang, Weiqi Li, Yanan Liu, Ruyi Zheng, Jiajia Wei, Shiju Ye, Yanmei Zhang, Bozhi Ye, Yi Wang, Huazhong Ying, Guang Liang

BACKGROUND: Pathological cardiac hypertrophy can result in heart failure. Protein dephosphorylation plays a primary role in the mediation of various cellular processes in cardiomyocytes. Here, we investigated the effects of a protein tyrosine phosphatase, PRL2 (phosphatase of regenerative liver 2), on pathological cardiac hypertrophy.

METHODS: The PRL2 knockout mice were subjected to angiotensin II infusion or transverse aortic constriction to induce myocardial hypertrophy and cardiac dysfunction. RNA-sequencing analysis was performed to explore the underlying mechanisms. Mass spectrometry and bio-layer interferometry assays were used to identify AMPKα2 (AMP-activated protein kinase α2) as an interacting protein of PRL2. Mutant plasmids of AMPKα2 were used to clarify how PRL2 interacts and dephosphorylates AMPKα2.

RESULTS: A significant upregulation of PRL2 was observed in hypertrophic myocardium tissues in mice and patients with heart failure. PRL2 deficiency alleviated cardiac hypertrophy, fibrosis, and dysfunction in mice challenged with angiotensin II infusion or transverse aortic constriction. Transcriptomic and biochemical analyses showed that PRL2 knockout or silence maintained AMPK^{T172} phosphorylation and subsequent mitochondrial integrity in angiotensin II-challenged heart tissues or cardiomyocytes. Mass spectrometry-based interactome assay indicated AMPKα2 subunit as the substrate of PRL2. Mechanistically, PRL2 binds to the C-terminal domain of AMPKα2 and then dephosphorylates AMPKα2^{T172} via its active site C46. Adeno-associated virus 9-mediated deficiency of cardiomyocyte PRL2 also protected cardiac mitochondrial function and showed cardioprotective effects in angiotensin II-challenged mice, but these benefits were not observed in AMPKα2$^{-/-}$ mice.

CONCLUSIONS: This study reveals that PRL2, as a novel AMPK-regulating phosphatase, promotes mitochondrial instability and hypertrophic injury in cardiomyocytes and provides PLR2 as a potential target for future drug development treating heart failure.

GRAPHIC ABSTRACT: A graphic abstract is available for this article.

Key Words: AMP-activated protein kinases ■ heart failure ■ hypertrophy ■ mitochondria ■ protein tyrosine phosphatases

Meet the First Author, see p 643 | Editorial, see p 664

One of the crucial precursor courses of heart failure (HF) is maladaptive myocardial hypertrophy, which results in subsequent myocyte fibrosis, chronic heart dysfunction, and even sudden death.[1] Increasing evidences have demonstrated that inflammation, calcium imbalance, oxidative stress, and impaired mitochondrial function are involved in the pathogenesis of myocardial hypertrophy.[2–4] Despite convincing progress in treating cardiovascular diseases, the mortality of HF remains high, creating an urgent need for new therapeutic targets

Correspondence to: Guang Liang, PhD, Hangzhou Medical College, Hangzhou, Zhejiang 310007, China, Email wzmcliangguang@163.com; or Huazhong Ying, MD, Hangzhou Medical College, Hangzhou, Zhejiang 310007, China, Email yhz0101@126.com
*X. Han and Q. Shi contributed equally.
Supplemental Material is available at https://www.ahajournals.org/doi/suppl/10.1161/CIRCRESAHA.124.325262.
For Sources of Funding and Disclosures, see page 662.

Circulation Research is available at www.ahajournals.org/journal/res

Novelty and Significance

What Is Known?

- Protein phosphorylation or dephosphorylation regulation plays a critical role in regulating the progression of cardiac hypertrophy and heart failure.
- AMPK (AMP-activated protein kinase) activation has been demonstrated as an effective strategy to preserve mitochondrial homeostasis and prevent cardiac hypertrophy.

What New Information Does This Article Contribute?

- The expression of a phosphatase, PRL2 (phosphatase of regenerative liver 2), is upregulated in both human and mouse hypertrophic myocardium, especially in cardiomyocytes.
- PRL2 deficiency or knockdown in cardiomyocytes prevents mitochondrial instability and subsequently cardiac hypertrophy and dysfunction in mouse models via activating AMPK.
- PRL2 inactivates AMPK via dephosphorylating AMPKα2 at threonine 172 through its active site of cysteine 46 in cardiomyocytes.

Understanding key protein tyrosine phosphatases in cardiac pathophysiology may provide new targets and strategies for the treatment of heart failure. Our study shows that PRL2 directly binds to AMPK, leading to the dephosphorylated AMPKα2 subunit at the T172 site to initiate mitochondrial changes in cardiomyocytes and then induce cardiac hypertrophy. Small-molecule PRL2 inhibitors may be a strategy to activate AMPK. Our findings suggest that PRL2 inhibition may be a future target for the treatment of heart failure.

Nonstandard Abbreviations and Acronyms

4-HNE	4-hydroxynonenal
8-OHdG	8-hydroxydeoxyguanosine
AAV9	adeno-associated virus 9
ACC	acetyl-CoA carboxylase
AMPK	AMP-activated protein kinase
Ang II	angiotensin II
ANP	atrial natriuretic peptide
ARPC	adult rat primary cardiomyocyte
CaMKK	calcium-activated calmodulin-dependent kinase kinase
CTD	C-terminal domain
Col1a1	collagen type I α 1 chain
FAO	fatty acid oxidation
HF	heart failure
LKB1	liver kinase B1
MYH7	myosin heavy chain 7
NRPC	neonatal rat primary cardiomyocyte
OXPHOS	oxidative phosphorylation
PGC-1α	peroxisome proliferator-activated receptor-γ coactivator-1α
PPARα	peroxidase proliferators activate receptor α
PRL2	phosphatase of regenerative liver 2
PTP	protein tyrosine phosphatase
TAC	transverse aortic constriction
TAK1	TGF-β-activated kinase-1
TGF-β1	transforming growth factor β1
VEGF	vascular endothelial growth factor
WT	wild type

for effective pharmacological interventions against cardiac hypertrophy.

Especially, HF and myocardial hypertrophy are commonly linked with cardiac energy disturbance because of the high energy demand by the heart.[5] The mitochondria offer the primary energy source to sustain cardiac excitation-contraction coupling, and this organelle is also involved in the production of ATP by oxidative phosphorylation (OXPHOS) and the maintenance of cellular capacity against oxidative stress.[6,7] Previous studies have shown that cardiac mitochondrial dysfunction and impaired mitochondrial biogenesis are positively associated with the progress of HF in patients and animal models.[6,8] It has been recently reported that activation of AMPK (AMP-activated protein kinase) ameliorates cardiac hypertrophy by modulating multiple processes such as mitochondrial energy metabolism, mitochondrial biogenesis, autophagy, fatty acid oxidation (FAO), and glucose metabolism.[9–11] AMPKα2 protects hearts against hypertrophy and contractile dysfunction via enhancing mitochondrial OXPHOS and improving mitochondrial function.[10] These reports suggest that maintaining

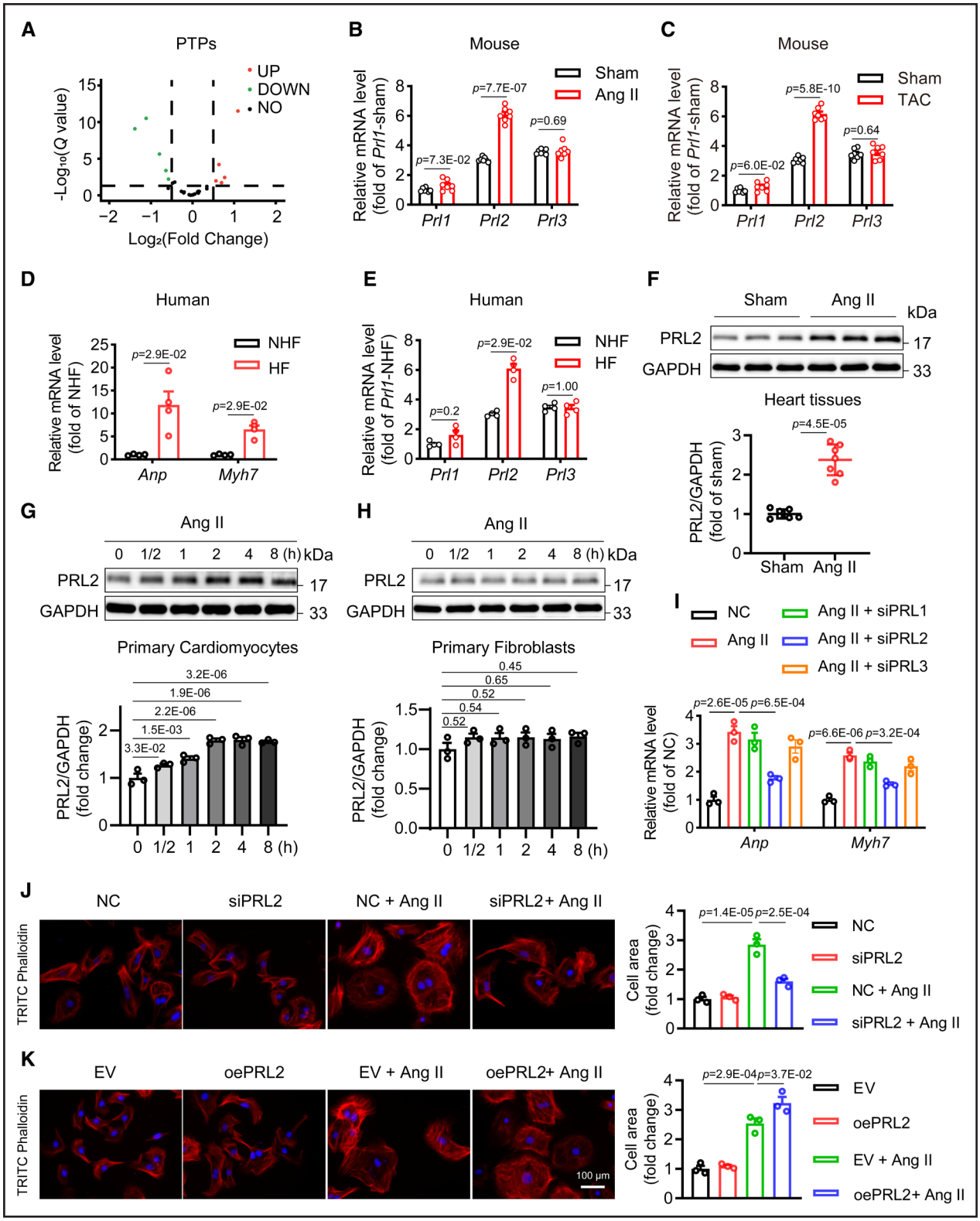

Figure 1. Upregulation of PRL2 level in cardiac hypertrophy.

A, RNA transcriptome sequencing was performed to analyze the expression profile of protein tyrosine phosphatases (PTPs) in angiotensin II (Ang II)-induced cardiac hypertrophy. Volcano plot of differentially expressed genes in heart tissues from control and Ang II-infusion mice. **B** and **C**, The mRNA levels of *Prl1*, *Prl2*, and *Prl3* in Ang II- or transverse aortic constriction (TAC)-treated mice. **D** and **E**, The mRNA levels of *Anp*, *Myh7*, *Prl1*, *Prl2*, and *Prl3* in patients with heart failure (HF; no heart failure [NHF]). **F**, Immunoblots analysis of PRL2 (phosphatase of regenerative liver 2) in Ang II-infused heart tissues and densitometric quantification. **G** and **H**, The protein levels of PRL2 in Ang II-induced neonatal rat primary cardiomyocytes (NRPCs) and primary fibroblasts. **I**, NRPCs were transfected with siRNA targeting PRL1, PRL2, or PRL3, then treated with 1 umol/L Ang II for 24 hours. Real-time quantitative polymerase chain reaction analysis mRNA levels of *Anp* and *Myh7*. **J** and **K**, (*Continued*)

AMPK activity and mitochondrial metabolism represents a promising therapeutic strategy for treating HF.

Protein phosphorylation plays critical roles in regulating the progression of HF.[12] The protein tyrosine phosphatases (PTPs) serve as counterbalance protein tyrosine kinases in response to signal transduction through dephosphorylating modification.[13] Phosphorylation modification can influence the activity, localization, and complex association of the functional proteins in cellular processes.[14] Therefore, deregulation of PTP expression or activity disrupts various signaling pathways and compromises cell physiological processes, leading to multiple disorders ranging from cancer to immune deficiencies and cardiovascular diseases.[14–16] In the past decade, despite new drugs on PTP-targeted treatment emerging for cancer therapy,[17,18] PTP-dependent therapeutics for cardiac diseases are still in the preliminary phase.[19] Discovering key PTPs in cardiac pathophysiology may provide new targets and strategies for the treatment of HF.

The PTP subfamily phosphatase of regenerative liver (PRL) comprises 3 members, including PRL1, PRL2, and PRL3, and possesses a conserved CAAX box at the C-terminal region and a single phosphatase domain that dephosphorylates the tyrosine and serine/threonine residues of kinases.[20] Compared with PRL1 and PRL3, PRL2 is broadly expressed and plays a prominent role in various pathophysiological processes.[21,22] For example, mice with PRL2 deletion exhibit limited angiogenesis and defective retinal vascular outgrowth.[23] However, the role of PRL2 in cardiac pathophysiology is poorly understood.

In this study, we examined the expression profile of all PTP genes in angiotensin II (Ang II)-infused mouse hearts, finding that PRL2 was significantly overexpressed. This phenomenon was further validated in a transverse aortic constriction (TAC)-induced cardiac hypertrophy mouse model and in patients with HF. PRL2 deficiency effectively prevented Ang II- or TAC-induced cardiac dysfunction and hypertrophy in mice. Interestingly, our mechanistic studies showed that PRL2 directly binds to AMPK and causes the dephosphorylated AMPKα2 subunit at the T172 site to initiate mitochondrial disorder in cardiomyocytes. These studies reveal a phosphatase, PRL2, as a new regulator in cardiac hypertrophy and HF.

METHODS

Data Availability

The data and detailed methods that support the findings of this study are described in the Supplemental Material and the Major Resources Table in the online supplementary files. The primers used for real-time quantitative polymerase chain reaction analysis are shown in Table S1. The experimental materials and analytical methods are also available from the corresponding author on reasonable request. Statistical analysis was performed as the Statistical Reporting Recommendations of *Circulation Research*.

RESULTS

Cardiomyocyte PRL2 Is Elevated in Pathological Cardiac Hypertrophy

To profile the variation of PTPs in the pathologically cardiac hypertrophy, we performed unbiased RNA-sequencing analysis in myocardium tissues of mice subjected to Ang II infusion. Among 107 PTP genes, we observed an abnormal expression of genes in the PRL subfamily in the Ang II infusion group (Figure 1A). We further examined the mRNA levels of PRLs (*Prl1*, *Prl2*, and *Prl3*) in Ang II-infused and TAC-treated mouse hearts, and interestingly, only *Prl2* mRNA was significantly elevated in heart tissues (Figure 1B and 1C). This finding was confirmed in myocardium tissues of human subjects who suffered from HF (Figure 1D and 1E; Table S2). Western blotting analysis showed that the protein level of cardiac PRL2 was much higher in Ang II-infused mice than that in the sham group (Figure 1F). Besides, Ang II increased PRL2 expression in neonatal rat primary cardiomyocytes (NRPCs) in a time-dependent manner, while no expression change was seen in primary fibroblasts (Figure 1G and 1H), indicating that increased PRL2 is mainly derived from the cardiomyocytes in the hearts of HF mice. Furthermore, the immunofluorescence staining using mouse heart samples verified that the PRL2 expression was upregulated in α-actinin-positive cardiomyocytes under Ang II infusion (Figure S1).

For functional examination of the PRLs family, we knocked down the PRLs in NRPCs (Figure S2A) and showed that deficiency in PRL2 (but not PRL1 and PRL3) significantly reduced Ang II-induced hypertrophic genes, including atrial natriuretic peptide (*Anp*) and myosin heavy 7 (*Myh7*; Figure 1I). Ang II stimulation also led to the increase in cardiomyocyte area, which was significantly reversed by transfection of siRNA (siPRL2; Figure 1J; Figure S2B). In contrast, overexpression of PRL2 through transfecting PRL2 plasmid in NRPCs aggravated Ang II-induced hypertrophic phenotypes (Figure 1K; Figure S2C and S2D). As expected, silencing PRL2 did not change the Ang II-induced increases of *TGF-β1* (transforming growth factor β1) and *Col1a1* (collagen type I α 1 chain) in fibroblasts (Figure S2E), indicating that PRL2 in fibroblasts does not mediate

Figure 1 Continued. TRITC-phalloidin staining in NRPCs, and the area of cardiomyocytes was quantified. Scale bar=100 μm. Data are shown as mean±SEM. **A**, **G**–**K**: n=3; **B**, **C**, and **F**: n=7; **D** and **E**: n=4; **B**, and **F**, Welch *t* test; **C**, Student *t* test; **D** and **E**, Mann-Whitney *U* test; **G**–**K**, 1-way ANOVA followed by Tukey post hoc tests; *P* values indicated. EV indicates empty vector; NC, negative control; oePRL2, over expression PRL2; and TRITC, tetramethylrhodamine.

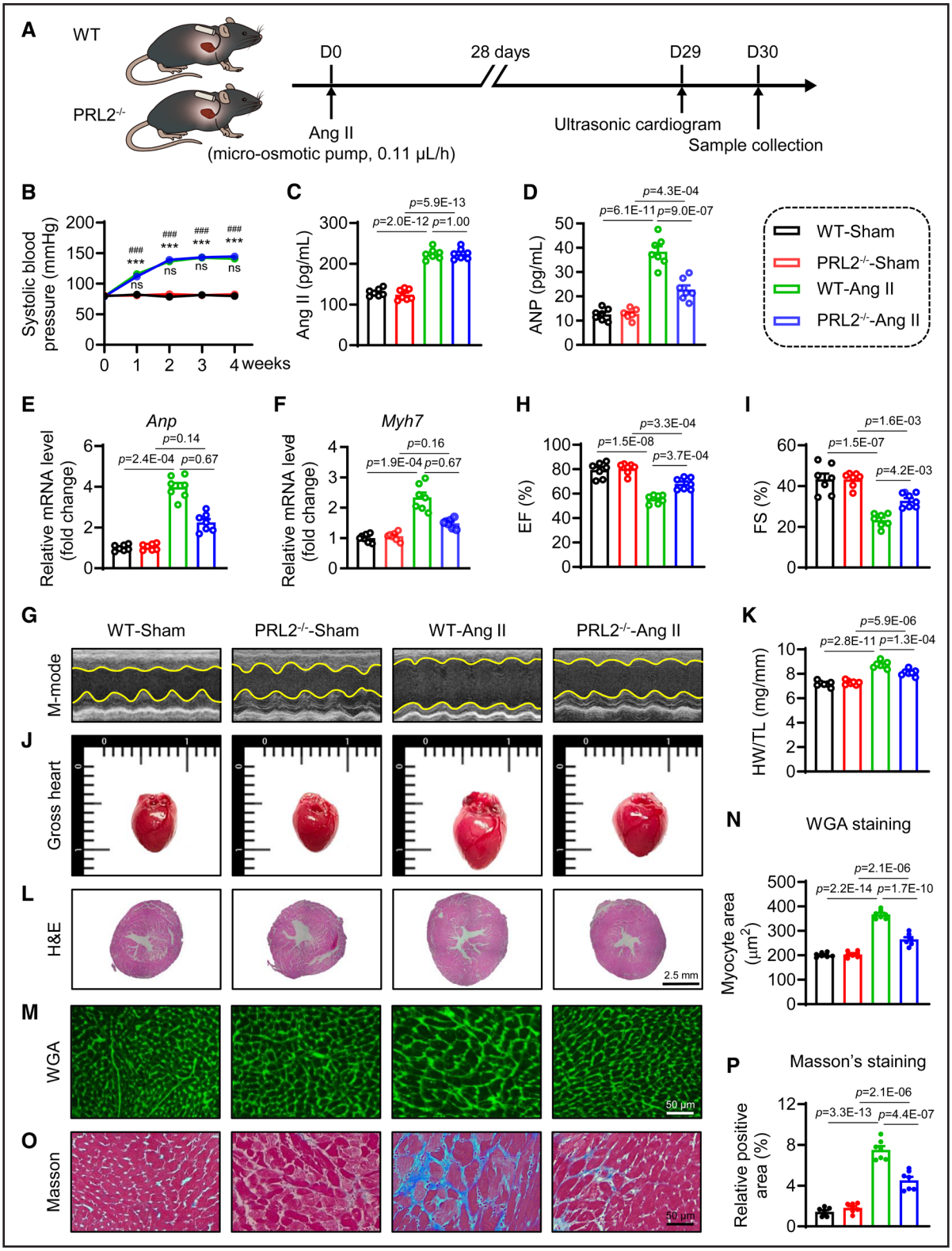

Figure 2. PRL2 (phosphatase of regenerative liver 2) deficiency alleviates angiotensin II (Ang II)-induced cardiac hypertrophy. **A**, Illustration of experimental protocols. The wild-type (WT) mice and PRL2 knockout (PRL2$^{-/-}$) mice were injected with Ang II via an osmotic pump for 28 days. After 4 weeks, the cardiac function of mice was assessed using echocardiography. Mice were then euthanized and samples were harvested. **B**, Mice systolic blood pressure was measured during the study. ***P<0.001 vs WT-Sham; ###P<0.001 vs PRL2$^{-/-}$-Sham; ns, no significance. **C** and **D**, Serum Ang II and atrial natriuretic peptide (ANP) levels were detected using ELISA kits. **E** and **F**, Real-time quantitative polymerase chain reaction analysis of mRNA levels of *Anp* and *Myh7* in cardiac tissues. **G**, Representative left ventricular M-mode echocardiographic images. **H** and **I**, Values of ejection fraction (EF) and fractional shortening (FS). **J**, Representative whole heart images. **K**, The ratio of heart weight to tibia length ratios (HW/TL). **L**, Representative images of hematoxylin and eosin (H&E) staining in (*Continued*)

profibrotic phenotypes. The pathological cardiomyocyte hypertrophy can activate cardiac fibroblasts and promote fibrosis via paracrine communications. We examined if cardiomyocyte PRL2 affects the activation of fibroblasts via intercellular crosstalk. We transfected NRPCs with siPRL2 or PRL2 plasmid and exposed them to Ang II for 24 hours, and the conditional medium of NRPCs was then collected and applied to primary mouse cardiac fibroblasts (Figure S2F). Our results showed that silencing PRL2 in cardiomyocytes significantly reduced the conditional medium-induced *TGF-β1* and *Col1a1* levels in fibroblasts (Figure S2G), while overexpressing PRL2 in cardiomyocytes exacerbated these changes in fibroblasts (Figure S2H). We also examined the effect of PRL2 in myocardial microvascular endothelial cells. Ang II reduced the mRNA level of vascular endothelial cadherin (*Cdh5*) and increased mesenchymal vimentin (*Vim*) and *Acat2*, while silencing PRL2 did not change the profile of these transcription factors associated with endothelial to mesenchymal transformation (EndMT; Figure S2I). Hence, these data suggest that PRL2 in cardiomyocytes seems to be related to cardiac hypertrophy.

PRL2 Deficiency Is Sufficient to Alleviate Ang II-Induced Cardiac Hypertrophy

To examine the function of PRL2 in Ang II-induced cardiac hypertrophy, the PRL2 knockout mice (PRL2$^{-/-}$) were constructed (Figure S3A). There was no detectable protein level of PRL2 in PRL2$^{-/-}$ mouse hearts (Figure S3B). The littermate wild-type (WT) mice and PRL2$^{-/-}$ mice were infused with Ang II at 1 μg/kg per min for 28 days to produce a well-established mouse model of pathological cardiac hypertrophy (Figure 2A). After Ang II infusion, the systolic blood pressure and the serum level of Ang II content were comparably risen in both WT and PRL2$^{-/-}$ mice (Figure 2B and 2C), indicating that loss of PRL2 does not influence the blood pressure and Ang II content in vivo. However, knockout of PRL2 diminished the serum concentration of ANP and the mRNA levels of *Anp* and *Myh7* in heart tissues of Ang II-challenged mice (Figure 2D and 2F). More importantly, a notable increase in cardiac performance was recorded in PRL2$^{-/-}$ mice compared with Ang II-challenged WT mice based on echocardiographic parameters, including ejection fraction and fractional shortening (Figure 2G through 2I; Table S3), and the decreases in the left ventricular internal diameter and interventricular septal thickness were also observed (Table S3), suggesting that PRL2 deletion protected systolic function in Ang II-infused mice. Consistent with echocardiography data, Ang II-challenged WT mice had larger hearts and a more increased heart weight to tibia length ratio than untreated WT mice, while PRL2 knockout significantly reversed these changes (Figure 2J and 2K; Table S3). Analysis of pathological changes in heart tissues showed remarkably hypertrophy and fibrosis in WT mice but not in PRL2$^{-/-}$ mice challenged with Ang II (Figure 2L through 2P; Figure S4). Therefore, knockout of PRL2 dramatically improves cardiac function and alleviates cardiac hypertrophy and fibrosis in Ang II-infused mice.

PRL2 Deficiency Prevents TAC-Induced Cardiac Hypertrophy

We also examined the function of PRL2 on cardiac hypertrophy using the TAC mouse model (Figure 3A). The significant elevations in serum ANP and mRNA levels of *Anp* and *Myh7* were detected in TAC-WT mice compared with sham mice, while PRL2 knockout did not show the TAC-induced increases (Figure 3B through 3D). Echocardiography assay showed that PRL2 deficiency preserved cardiac function in TAC mice (Figure 3E through 3G; Table S4). Cardiac hypertrophy and fibrosis in TAC mice were also markedly decreased by PRL2 knockout (Figure 3H through 3N; Figure S5A through S5C), along with the significantly reduced expression of *TGF-β1* and *Col1a1* in TAC-induced PRL2$^{-/-}$ mice compared with WT mice (Figure S5D and S5E).

PRL2 Deficiency Rescues AMPK Activation and Alleviates Mitochondrial Injury in Ang II-Challenged Mouse Heart

To identify the molecular mechanism underlying PRL2-mediated cardiac hypertrophy, we performed RNA-sequencing analysis in the hearts of Ang II-challenged WT and PRL2$^{-/-}$ mice. A total of 948 genes were downregulated and 294 genes were upregulated after Ang II infusion in PRL2 deficient heart tissues (Figure S6A). Interestingly, gene set enrichment analysis found that the pathway of AMPK was affected by PRL2 deficiency in Ang II-challenged hearts (Figure 4A). We then examined the potential effects of PRL2 on AMPK phosphorylation at 3 probable phosphorylation sites (T172, S491, and S173) using a public proteomic database (Table S5).[24] Interestingly, Ang II infusion significantly inhibited the phosphorylation of AMPK at T172, but not at S491 and S173, while PRL2 knockout reduced Ang II-induced AMPK dephosphorylation at T172 and AMPK activity in the heart, indicating the regulation of AMPK activity by PRL2 (Figure 4B; Figure S6B and S6C).

Figure 2 Continued. heart samples (transverse). Representative images and quantitative analysis for wheat germ agglutinin (WGA; **M** and **N**) and Masson (**O** and **P**) staining. Scale bar=2.5 mm for H&E; 50 μm for WGA and Masson. Data are shown as mean±SEM. N=7; **B**, 2-way ANOVA followed by Tukey post hoc tests; **C**, **D**, **H**, **I**, **K**, **N**, and **P**, 1-way ANOVA followed by Tukey post hoc tests; **E** and **F**, Kruskal-Wallis test with Dunn post hoc tests; *P* values indicated.

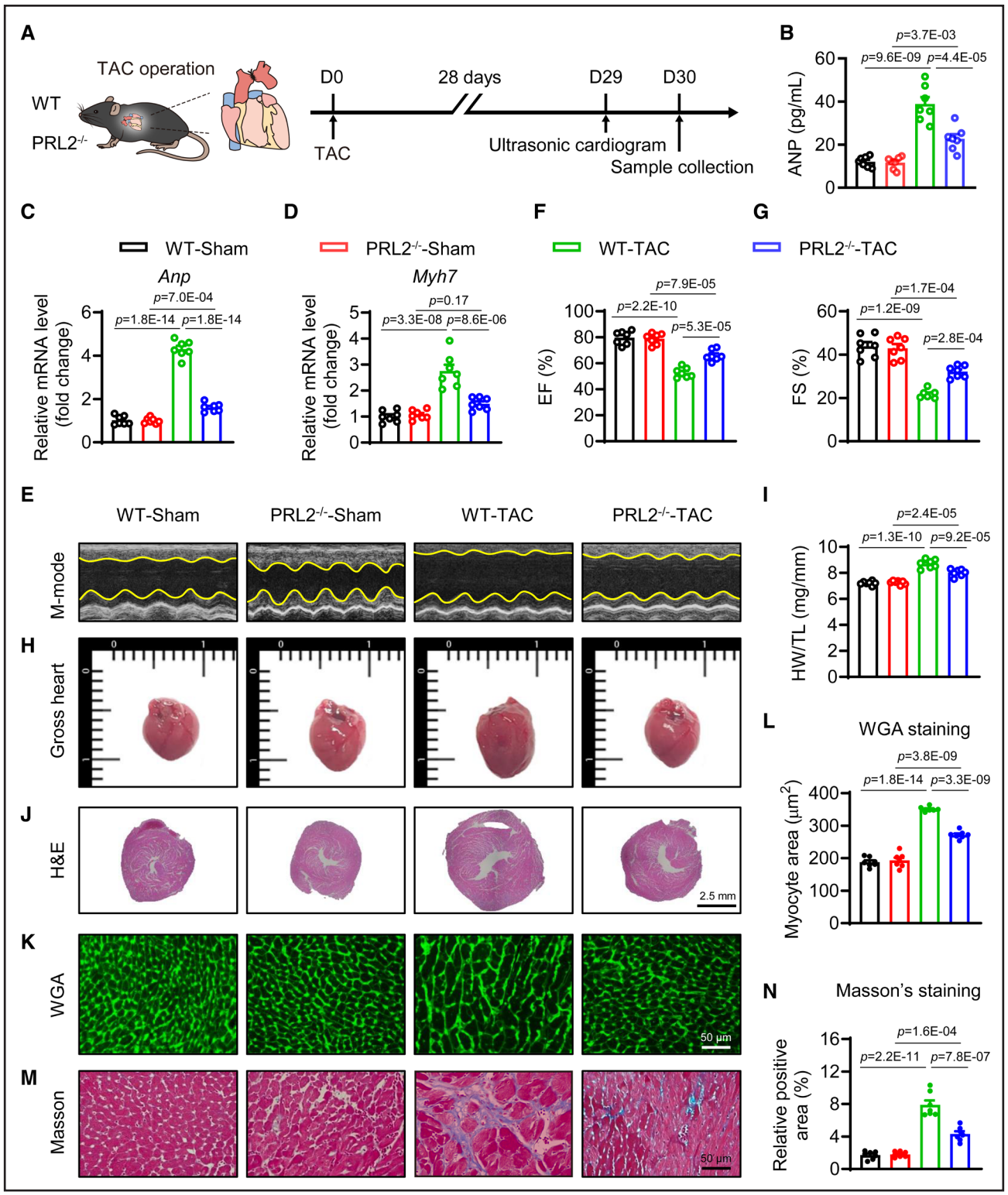

Figure 3. PRL2 (phosphatase of regenerative liver 2) knockout ameliorates transverse aortic constriction (TAC)-induced cardiac hypertrophy.

A, Illustration of experimental design for TAC-induced cardiac remodeling model. **B**, The concentration of atrial natriuretic peptide (ANP) in serum. **C** and **D**, The mRNA levels of *Anp* and *Myh7* were detected by real-time quantitative polymerase chain reaction in heart tissues. **E**, Representative M-mode echocardiographic images in TAC-induced mice. **F** and **G**, Ejection fraction (EF) and fractional shortening (FS) values in all groups. **H**, Representative whole heart images. **I**, The ratio of heart weight to tibia length ratios (HW/TL). **J** through **L**, Size of myocardial cells was evaluated with hematoxylin and eosin (H&E) and wheat germ agglutinin (WGA) staining in heart samples. **M** and **N**, The degree of fibrosis was analyzed with Masson staining. Scale bar=2.5 mm for H&E; 50 μm for WGA and Masson. Data are shown as mean±SEM. N=7; **B**–**D**, **F**, **G**, **I**, **L**, and **N**, 1-way ANOVA followed by Tukey post hoc tests; *P* values indicated.

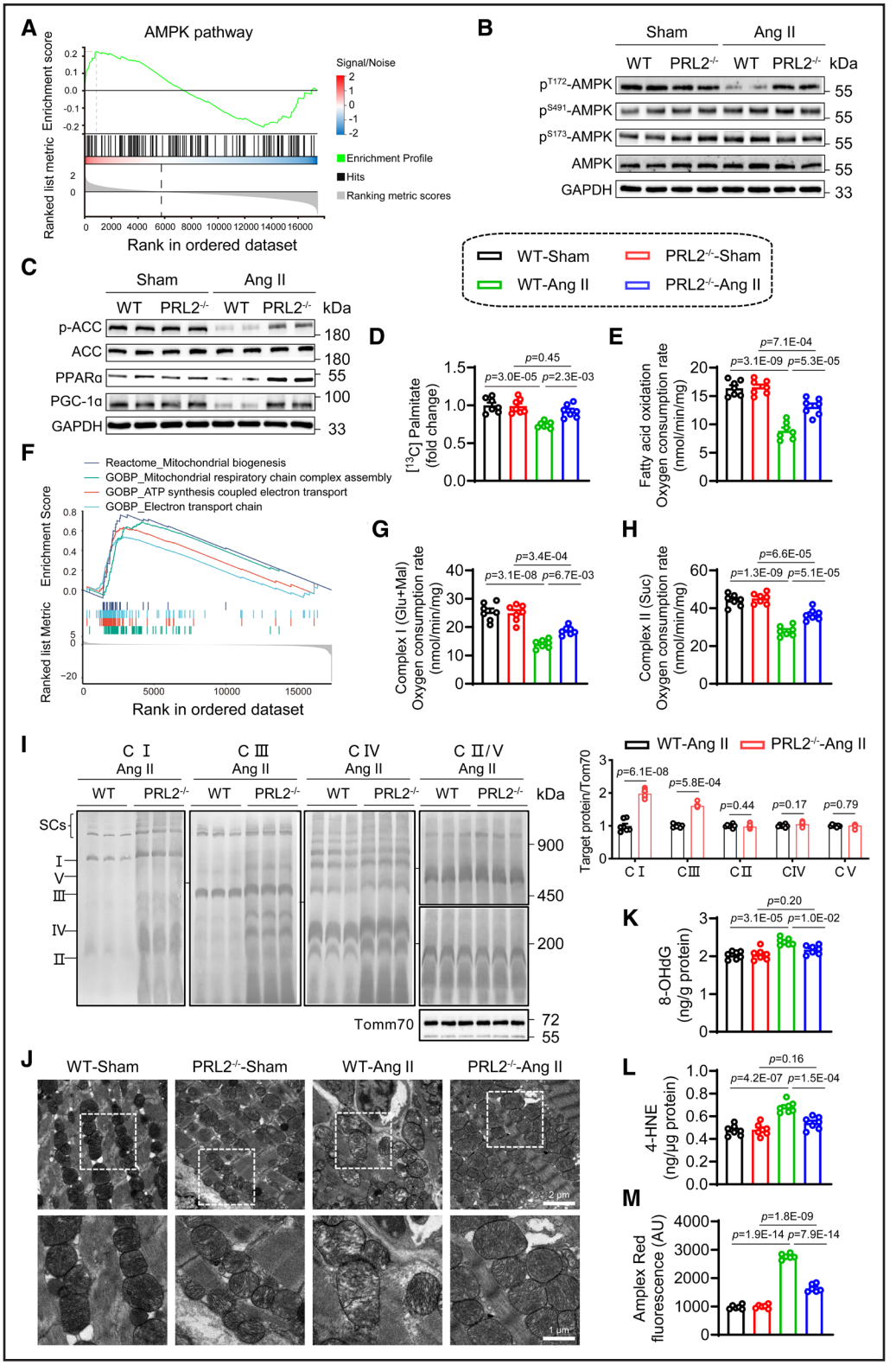

Figure 4. PRL2 (phosphatase of regenerative liver 2) deficiency maintains AMPK (AMP-activated protein kinase) phosphorylation and protects mitochondrial function in angiotensin II (Ang II)-challenged mouse hearts.

A and **B**, Pathway enrichment analysis related to AMPK pathway in heart tissues of the wild-type (WT)-Ang II and PRL2$^{-/-}$-Ang II mice based on RNA-sequencing data. **B**, Western blotting analysis of phosphorylated AMPK at different sites in heart tissues. **C**, Western blotting analysis of proteins associated with fatty acid oxidation (FAO) and mitochondrial biogenesis. **D**, The fold change of fractional enrichment of acetyl-coenzyme A (CoA) from ^{13}C-labeled palmitate into the transverse aortic constriction cycle in the isolated mouse heart. **E**, FAO was measured by oxygen consumption with octanoylcarnitine in adult mouse primary cardiomyocytes (AMPCs). **F**, Pathway enrichment analysis related to mitochondrial homeostasis in PRL2$^{-/-}$ heart tissues compared with WT heart tissues. **G** and **H**, Oxygen consumption by mitochondrial complex I (*Continued*)

Acetyl-CoA carboxylase (ACC) and PPARα (peroxisome proliferator-activated receptor α) are known as the downstream substrates/signals of AMPK and are involved in accelerating FAO in cardiomyocytes.[9,25] The gene ontology biological process analyses of our RNA-sequencing data also showed that the fatty acid metabolism-related process was enriched (Figure S6D and S6E), and the fatty acid metabolism pathways were significantly upregulated by PRL2 deficiency. In Ang II infusion mice, PRL2 knockout caused higher levels of p-ACC and PPARα in heart tissues than that of WT mice (Figure 4C; Figure S6F). We further evaluated the fatty acid metabolism and FAO respiration in vivo. The mouse hearts were perfused with 13C-palmitate to assess fatty acid metabolism, as previously reported.[26] The contribution of carbon derived from palmitate entry into the Krebs cycle was much greater in Ang II-challenged PRL2$^{-/-}$ mouse hearts than that in WT hearts, suggesting a high level of fatty acid utilization in PRL2$^{-/-}$ hearts (Figure 4D). In addition, Ang II challenge impaired the FAO respiratory in adult mouse primary cardiomyocytes with malate and octanoylcarnitine, while this change was reversed by PRL2 knockout (Figure 4E).

AMPK has been reported to regulate mitochondrial function and subsequent oxidative stress in cardiomyocytes.[10] Gene set enrichment analysis also found that the pathways of mitochondrial biogenesis and mitochondrial respiratory chain were affected by PRL2 deficiency in Ang II-challenged hearts (Figure 4F; Figure S6G). Consistent with the gene set enrichment analysis results, upregulated expression of PGC-1α (peroxisome proliferator-activated receptor-γ coactivator-1α) was observed in heart tissues from Ang II-infused PRL2$^{-/-}$ mice (Figure 4C; Figure S6F). Meanwhile, Ang II-challenged WT mouse heart tissues had lower mitochondrial DNA content than the PRL2$^{-/-}$ hearts (Figure S6H). In addition, mitochondrial oxygen consumption was detected in isolated mitochondria from heart tissues. The complex I and II-mediated mitochondrial respiration was significantly impaired in the hearts of Ang II-challenged mice, while an improvement of mitochondrial oxygen consumption was observed in PRL2$^{-/-}$ mouse hearts (Figure 4G and 4H). Moreover, the steady-state levels of mitochondrial complex I and III were much higher in heart tissues of PRL2$^{-/-}$ mice than that of WT mice with Ang II infusion, while the levels of mitochondrial complex II, IV, and V remained unaffected (Figure 4I). We further performed electron microscopy and found mitochondrial swelling, mitochondrial ridge disappearance, and increased mitochondrial size in heart tissues from Ang II-infused WT mice, while PRL2$^{-/-}$ mice mitigated these changes (Figure 4J; Figure S6I and S6J). We applied a modified 5-grade scorning system to evaluate mitochondrial damage,[27] and the score showed that PRL2 knockout effectively improved Ang II-induced mitochondrial damage in heart tissues (Figure S6K). Ang II decreased the mitochondrial membrane potential in adult mouse primary cardiomyocytes from WT mice, while adult mouse primary cardiomyocytes from PRL2 knockout mice showed a resistance against this Ang II-induced change (Figure S6L and S6M). To assess oxidative stress changes, we detected the levels of 8-hydroxydeoxyguanosine (8-OHdG), an indicator of DNA damage, and 4-hydroxynonenal (4-HNE), a product of lipid peroxidation. High levels of 8-OHdG and 4-HNE were decreased by PRL2 deficiency in Ang II-challenged heart tissues (Figure 4K and 4L). Ang II-induced H_2O_2 emissions indicated by Amplex Red fluorochrome were also significantly reduced by PRL2 knockout in adult mouse primary cardiomyocytes (Figure 4M).

Similarly, PRL2 knockout alleviated TAC-induced AMPK^{T172} dephosphorylation, downregulation of p-ACC, PPARα, PGC-1α, and fatty acid metabolism, and upregulation of 8-OHdG and 4-HNE in heart tissues (Figure S7). PRL2 deletion in endothelial cells has been reported to limit retinal vascular outgrowth and sprouting angiogenesis in mice.[23] Then, we examined the possible role of PRL2 in cardiac angiogenesis. RNA-sequencing-based pathway enrichment analysis showed that PRL2 deficiency failed to affect the enrichment of angiogenesis-related signals in Ang II-infused mouse heart tissues (Figure S8A through S8D). In addition, immunofluorescence staining for the endothelial marker CD31 showed that PRL2 knockout did not affect Ang II-induced CD31 expression in mouse heart tissues (Figure S8E). These results deny the involvement of PRL2 in cardiac angiogenesis in Ang II-infused mice. Taken together, these results indicate that PRL2 deficiency rescues AMPK phosphorylation and subsequently alleviates mitochondrial injury in Ang II- and TAC-challenged myocardium.

PRL2 Mediates Ang II-Induced AMPK Inactivation and Mitochondrial Injury in Cardiomyocytes

We further evaluated the effects of PRL2 on AMPK phosphorylation and mitochondrial homeostasis in NRPCs. Silencing PRL2 in NRPCs dramatically increased the phosphorylation at T172 of AMPK and p-ACC upon Ang II stimulation, concurrent with significantly increased

Figure 4 Continued. and complex II in mitochondria isolated from heart tissues. **I**, Western blotting analysis of mitochondrial respiratory complex and densitometric quantification. **J**, Representative electron microscopic images of heart sections. **K** and **L**, The levels of 8-hydroxydeoxyguanosine (8-OHdG) and 4-hydroxynonenal (4-HNE) were detected by ELISA kits. **M**, H_2O_2 emissions were measured by Amplex Red fluorochrome in AMPCs. Scale bar=2 μm (**top**) and 1 μm (**bottom**) for electron microscopic images. Data are shown as mean±SEM. **A** and **F**: n=4; **B**–**E**, **G**–**M**: n=7; **D**, **E**, **G**, **H**, and **K**–**M**, 1-way ANOVA followed by Tukey post hoc tests; I, Student *t* test; I (**C**, III), Mann-Whitney *U* test; *P* values indicated. ACC indicates acetyl-CoA carboxylase; p-ACC, phosphorylated-acetyl-CoA carboxylase; PGC-1α, peroxisome proliferator-activated receptor-γ coactivator-1α; and PPARα, peroxidase proliferators activate receptor α.

ORIGINAL RESEARCH

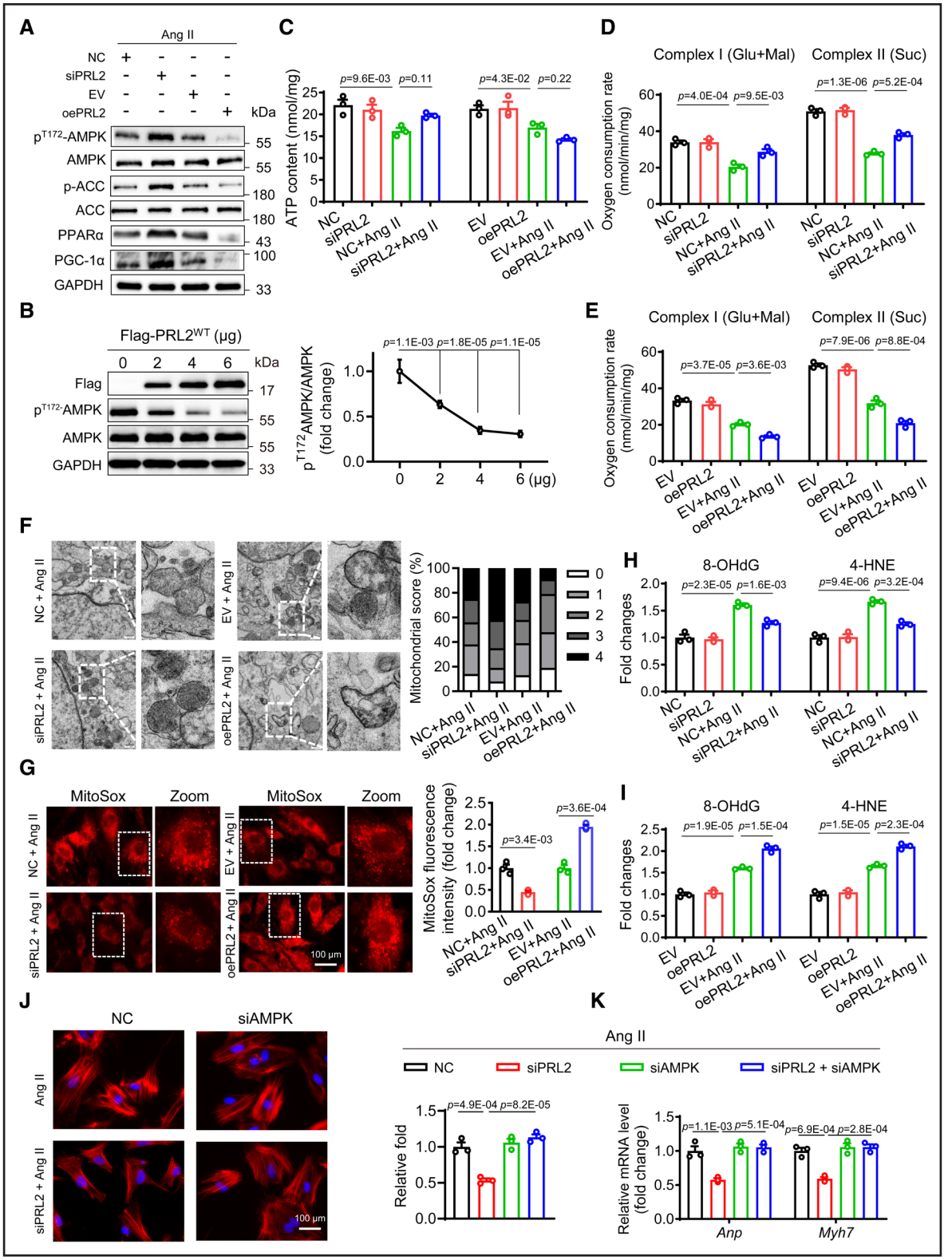

Figure 5. PRL2 (phosphatase of regenerative liver 2) mediates angiotensin II (Ang II)-induced AMPK (AMP-activated protein kinase) inactivation and mitochondrial dysfunction in cardiomyocytes.

Neonatal rat primary cardiomyocytes (NRPCs) were transfected with siRNA targeting PRL2 or negative control (NC), or with a plasmid encoding PRL2 or empty vector (EV) before Ang II stimulation. **A**, Western blotting analysis of p^{T172}-AMPK, AMPK, p-ACC (phosphorylated-acetyl-CoA carboxylase), acetyl-CoA carboxylase (ACC), PPARα (peroxidase proliferators activate receptor α), and PGC-1α (peroxisome proliferator-activated receptor-γ coactivator-1α) in NRPCs. **B**, Hek293T cells were transfected with various amounts of Flag-PRL2. Western blotting analysis (**left**) and densitometric quantification (**right**) of PRL2. **C**, ATP contents in NRPCs. **D** and **E**, Oxygen consumption by mitochondrial complex I and complex II in NRPCs. **F**, Representative transmission electron micrographs of NRPCs, and mitochondrial scores were analyzed. (*Continued*)

levels of PPARα and PGC-1α (Figure 5A; Figure S9A and S9B). By contrast, increased protein expression of the PRL2 via transfection of PRL2 plasmid in NRPCs significantly reduced the levels of p^{T172}-AMPK, p-ACC, PPARα, and PGC-1α under Ang II treatment (Figure 5A; Figure S9A and S9B). Consistently, neither knockdown nor overexpression of PRL2 affected the levels of p^{S491}-AMPK and p^{S173}-AMPK in NRPCs (Figure S9C). In HEK-293T cells, the reduced levels of p^{T172}-AMPK were correlated with increased protein levels of PRL2, further validating that PRL2 dephosphorylates AMPK at T172 (Figure 5B). Moreover, we found that silencing PRL1 or PRL3 could not affect AMPK phosphorylation at T172 in NRPCs with or without Ang II challenge (Figure S9D).

Subsequently, we examined the AMPK-downstream mitochondrial phenotypes in NRPCs. Silencing PRL2 significantly increased ATP production (Figure 5C), complex I and II-mediated mitochondrial respiration (Figure 5D), intracellular basal mitochondrial respiration, proton leakage-associated respiration, and maximal respiration in Ang II-challenged NRPCs (Figure S9E). In contrast, these parameters were further reduced in NRPCs stably overexpressing PRL2 (Figure 5C and 5E; Figure S9F). In parallel, PRL2 knockdown alleviated the Ang II-induced mitochondrial morphology damage (Figure 5F) and mitochondrial reactive oxygen species, 8-OHdG, and 4-HNE levels in NRPCs (Figure 5G and 5H; Figure S9G and S9H), while overexpression of PRL2 aggravated these parameters in Ang II-challenged NRPCs (Figure 5F, 5G, and 5I; Figure S9G and S9H). Finally, we examined whether PRL2 affected Ang II-induced cardiac hypertrophy through regulating AMPK activity in cardiomyocytes. As shown in Figure 5J, AMPK knockdown by siRNA significantly reversed siPRL2-decreased cardiomyocyte area. Similarly, AMPK knockdown by siRNA also abolished the reduction of hypertrophic gene expression by siPRL2 treatment in Ang II-challenged NRPCs (Figure 5K). These results confirm that PRL2 regulates AMPK activity and mitochondrial damage to induce hypertrophy in cardiomyocytes.

PRL2 Directly Interacts with the C-Terminal Domain of AMPKα2 and Dephosphorylates AMPKα2 at T172 via Its Active Site C46

To identify the detailed mechanism and potential targets by which PRL2 regulates AMPK dephosphorylation, we analyzed the PRL2 interactome by immunoprecipitation and mass spectrometry assay for 3× (interactome workflow shown in Figure 6A). Through comparing these 3 interactomes, we identified 5 potential substrates of PRL2, including Prkaa2 (AMPKα2), C1qbp, Atad3a, Rpl10a, and Rpn1 (Figure 6A). Among these 5 candidate proteins, AMPKα2, C1qbp, and Atad3a have been reported to participate in cardiomyocyte pathophysiology[28,29] (Table S6). Therefore, we examined the endogenous interaction of PRL2 with these 3 potential substrates in cardiomyocytes. We confirmed the interactions of PRL2 with AMPK and Atad3a in Ang II-induced NRPCs, but there was no interaction between PRL2 and C1qbp (Figure 6B and 6C; Figure S10A and S10B). Interestingly, the interaction between PRL2 and Atad3a disappeared when AMPKα2 was deleted in NRPCs (Figure S10A), suggesting that the PRL2-Atad3a interaction depends on AMPKα2. These data indicate that AMPK, but not C1qbp or Atad3a, is the main substrate of PRL2 in cardiomyocytes. We then examined the PRL2-AMPK interaction in heart tissues (Figure 6D). We also used a bio-layer interferometry assay to confirm the direct interaction between rhPRL2 and rhAMPK proteins, with an association constant (KD) of 1.09×10^{-8} M (Figure 6E).

Structurally, AMPK, as an obligate heterotrimer, is composed of a catalytic subunit α (α1 or α2) and 2 noncatalytic subunits β (β1or β2) and γ (γ1, γ2, or γ3) subunits. It has been reported that AMPKα2, β1, β2, γ1, and γ2 are expressed in the mammal heart.[10] We constructed the plasmids for HA-tagged AMPKα1, α2, β1, β2, γ1, and γ2 subunits and cotransfected the Flag-tagged PRL2 and different AMPK subunit plasmids in HEK-293T cells. It was shown that PRL2 only bound to AMPKα1 and α2 but not other subunits (Figure 6F; Figure S10C). However, when we assessed the interaction of endogenous PRL2 and AMPK subunit α (α1 and α2) in NRPCs, we found that PRL2 predominantly bound to AMPKα2 but not α1, as the total AMPK α1 protein level is low in cardiomyocytes (Figure S10D and S10E). We further showed that silencing AMPKα1 did not affect PRL2-induced upregulation of *Anp* and *Myh7* mRNAs in Ang II-challenged NRPCs (Figure S10F). These data promote us to further validate the AMPKα2-PRL2 interaction in cardiomyocytes. Immunofluorescence staining further demonstrated endogenous PRL2 and AMPKα2 showed obvious colocalization in NRPCs upon Ang II exposure (Figure 6G). Coimmunoprecipitation assay using HEK-293T cells with Flag-tagged PRL2 and

Figure 5 Continued. **G**, Representative images and quantitative analysis of MitoSox staining. **H** and **I**, The levels of 8-hydroxydeoxyguanosine (8-OHdG) and 4-hydroxynonenal (4-HNE) in NRPCs. **F**, ATP content in the NRPCs. **G** and **H**, Oxygen consumption rate in the NRPCs. The base represents basal mitochondrial respiration; oligomycin (oligo) represents uncoupled mitochondrial respiration, and carbonyl cyanide 4-(trifluoromethoxy) phenylhydrazone (FCCP) represents uncoupled mitochondrial respiration, measured in the presence of oligomycin (2 μg/mL). **J**, NRPCs were transfected with siPRL2 or AMPK knockdown by siRNA (siAMPK) before exposure to Ang II for 24 hours. TRITC-phalloidin staining of NRPCs and the area of cardiomyocytes were quantified. **K**, The mRNA levels of *Anp* and *Myh7* were detected by real-time quantitative polymerase chain reaction in NRPCs. Scale bar=500 nm for electron microscopic images; 100 μm for MitoSox; 100 μm for TRITC-phalloidin. Data are shown as mean±SEM. N=3; **G**, Student *t* test; **B**–**E** and **H**–**K**, 1-way ANOVA followed by Tukey post hoc tests; *P* values indicated. oePRL2 indicates over expression PRL2.

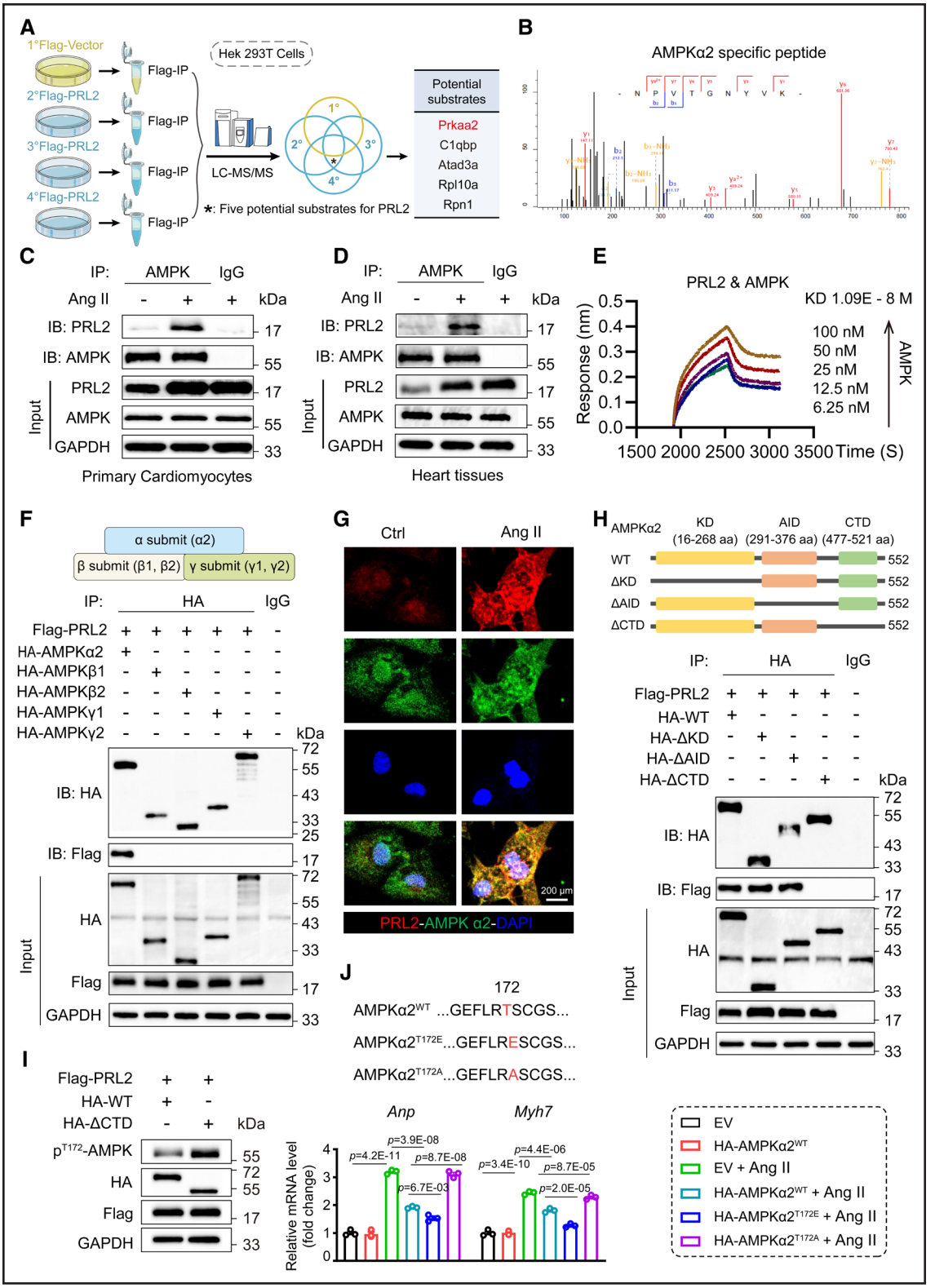

Figure 6. Identification of AMPKα2 (AMP-activated protein kinase) as a substrate of PRL2 (phosphatase of regenerative liver 2). **A**, Schematic of the quantitative proteomic screen to identify proteins binding to PRL2. **B**, Tandem mass spectrometry (MS/MS) spectrum of the specific peptide (-NPVTGNYVK-) from AMPKα2. **C** and **D**, Coimmunoprecipitation of PRL2 and AMPK in neonatal rat primary cardiomyocytes (NRPCs) and heart tissues. **E**, Bio-layer interferometry analysis showing the interaction between PRL2 and recombinant AMPK protein. AMPK was added at different concentrations ranging from 6.25 to 100 nmol/L, and kinase domain (KD) values were calculated. **F**, Coimmunoprecipitation of PRL2 and different subunits of AMPK in Hek293T cells. **G**, Representative images of immunofluorescence staining for PRL2 (red) and AMPKα2 (green) in NRPCs. **H**, Illustration of the AMPKα2 domain deletion construct, and coimmunoprecipitation of PRL2 and wild-type (WT)-AMPKα2 or mutants-AMPKα2 in Hek293T cells. **I**, Hek293T cells cotransfected with Flag-PRL2 and HA-WT-(*Continued*)

HA-tagged AMPKα2 plasmids confirmed this interaction (Figure S10G and S10H). Furthermore, mapping the domain of AMPKα2 required for PRL2 binding showed that the C-terminal domain (CTD; AA477–AA521) was critical for the interaction with PRL2 (Figure 6H). When deleting the CTD region in AMPKα2, PRL2 failed to dephosphorylate AMPK at T172 (Figure 6I), indicating that the PRL2-AMPKα2 interaction affords the dephosphorylating regulation of PRL2 on AMPK^{T172}. Taken together, these evidences indicate that PRL2 binds to AMPKα2 directly via its CTD, which subsequently results in the dephosphorylation of AMPK at the T172 site.

To further evaluate the effects of AMPK^{T172} phosphorylation on cardiac hypertrophy, we constructed a gain-of-function mutant plasmid (AMPKα2^{T172E}) or loss-of-function mutant plasmid (AMPKα2^{T172A}) and transfected them in NRPCs (Figure S10I). Overexpression of AMPKα2^{WT} inhibited Ang II-induced mRNA levels of hypertrophic genes *Anp* and *Myh7* in NRPCs. The autoactivated mutation, AMPKα2^{T172E}, further decreased Ang II-induced *Anp*/*Myh7* expression than AMPKα2^{WT}, while the inactive mutation AMPKα2^{T172A} failed to affect Ang II-induced gene expression (Figure 6J). These results suggest that AMPKα2 phosphorylation at T172 plays a key role in preventing PRL2-mediated cardiac hypertrophy.

It has been reported that the C46, D69, and C101 residues in the PTP domain of the PRL2 protein are the active sites supporting the phosphatase activity of PRL2.[21] We constructed WT, C46A, D69A, and C101A variants of PRL2, respectively, and transfected these plasmids into HEK293T cells. As shown in Figure 7A, only the C46A mutation failed to reduce the phosphorylation of AMPK^{T172}. These data indicate that the C46 site, a residue evolutionarily conserved across species (Figure 7B), is the critical residue for PRL2 activity regulating AMPK. We then examined whether the C46A mutation would also diminish the effects of PRL2 on subsequent mitochondrial injury and hypertrophy in cardiomyocytes. We expressed the PRL2^{WT} or PRL2^{C46A} in NRPCs, where the basal PRL2 protein had been deleted by siRNA. Ang II stimulation inhibited the mitochondrial OXPHOS and increased *Anp*/*Myh7* expression in PRL2^{WT} NRPCs, while the C46A mutation in PRL2^{C46A} NRPCs significantly reversed these changes induced by Ang II (Figure 7C and 7D). Collectively, these lines of mechanistic studies show that PRL2 directly interacts with the CTD of AMPKα2 and then dephosphorylates AMPK at the T172 site via its active residue C46, resulting in subsequent mitochondrial injury and hypertrophy in cardiomyocytes (Figure 7E).

AMPKα2 Knockout Diminishes the Cardioprotective Effects of PRL2 Deficiency in Ang II-Challenged Mice

To validate whether PRL2 deficiency protects hearts through regulating AMPKα2 in mice, we used WT and AMPKα2 knockout (AMPKα2$^{-/-}$) mice and injected them with recombinant adeno-associated virus 9 (AAV9) vector carrying PRL2 shRNA (AAV9-shPRL2) to silencing PRL2 in mouse hearts (Figure 8A). The efficacy of the AMPKα2 knockout and AAV9-shPRL2-mediated PRL2 knockdown in mouse hearts was confirmed at the protein level (Figure S11A and S11B). PRL2 knockdown induced by AAV9-shPRL2 did not affect the protein levels of AMPKα1, AMPKα2, and total AMPK in mouse hearts, while AMPKα1 level showed a slight and compensatory upregulation in AMPKα2$^{-/-}$ mice (Figure S11B). However, because the level of AMPKα1 was much lower than AMPKα2 in hearts (Figure S10D), the compensatory upregulation of AMPKα1 failed to change the overall situation of AMPK, and the total AMPK remains significantly downregulated in AMPKα2$^{-/-}$ mice compared with WT mice (Figure S11B). Neither AMPKα2 knockout nor PRL2 knockdown affected the Ang II-induced blood pressure profile in mice (Figure 8B). The content of serum ANP and the mRNA levels of cardiac *Anp* and *Myh7* indicated that AAV9-mediated PRL2 knockdown in hearts significantly blunted Ang II-induced myocardial hypertrophy in WT mice (Figure 8C through 8E). However, knockdown of PRL2 failed to reduce *Anp*/*Myh7* levels in AMPKα2$^{-/-}$ mice (Figure 8C through 8E). Echocardiography assay also showed that PRL2 knockdown reversed Ang II-induced heart dysfunction in the WT mice but failed in AMPKα2$^{-/-}$ mice (Figure 8F through 8H; Table S7). Examination on the ratio of heart weight to tibia length and morphological analyses showed that AAV9-shPRL2 injection attenuated cardiac hypertrophy in Ang II-challenged WT mice (Figure 8I through 8M; Table S7). Masson and Sirius red staining revealed that AAV9-shPRL2 also attenuated Ang II-induced cardiac fibrosis in WT mice (Figure S12). However, PRL2 knockdown in hearts showed no effects against Ang II-induced fibrosis when AMPKα2 is deficient in mice (Figure S12). Finally, the upregulated AMPK^{T172} and ACC phosphorylation, PPARα, and PGC-1α were observed in the heart tissues of AAV9-shPRL2-infected WT mice, while these changes were not observed in AMPKα2$^{-/-}$ mice (Figure S13A). Subsequently, AAV9-shPRL2 treatment improved mitochondrial morphology and injury of cardiomyocytes in WT mice but not in AMPKα2$^{-/-}$ mice

Figure 6 Continued. AMPKα2 or HA-CTD deletion-AMPKα2. Western blotting analysis of p^{T172}-AMPK level. **J**, Schematic of the AMPKα2 phosphorylated threonine residue variant (T172E and T172A). Real-time quantitative polymerase chain reaction of *Anp* and *Myh7* in lysates of NRPCs transfected with WT-AMPKα2 or AMPKα2 mutant vectors, and then challenged with angiotensin II (Ang II) for 24 hours. Scale bar=200 μm. Data are shown as mean±SEM. **A**, n=4; **C**–**J**, n=3; **J**, 1-way ANOVA followed by Tukey post hoc tests; *P* values indicated. AID indicates autoinhibitory sequence domain; CTD, carboxyl-terminal domain; EV, empty vector; and HA, hemagglutinin.

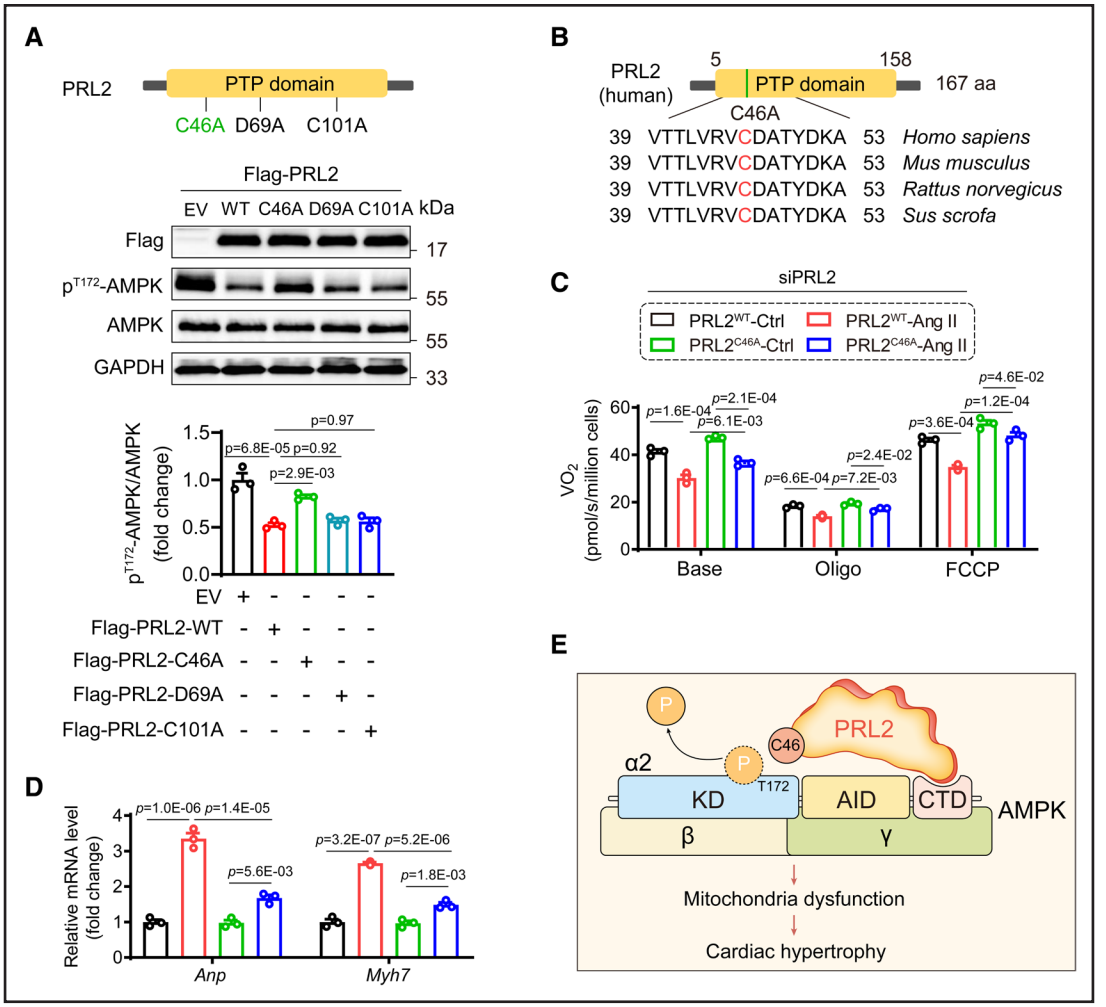

Figure 7. PRL2 (phosphatase of regenerative liver 2) dephosphorylates AMPKα2^{T172} (AMP-activated protein kinase) via its enzyme active site C46.

A, Western blotting analysis of p^{T172}-AMPK and AMPK in Hek293T cells cotransfected with wild-type (WT) or mutation of enzyme active sites of PRL2 plasmids (**top**) and densitometric quantification (**bottom**). **B**, Clustal alignment of conserved sites in PRL2. **C**, Neonatal rat primary cardiomyocytes (NRPCs) were transfected with siRNA targeting PRL2, cotransfected with a plasmid encoding PRL2-WT or PRL2-C46A, then stimulated with angiotensin II (Ang II). Oxygen consumption rate measured in the NRPCs. The base represents basal mitochondrial respiration; oligomycin (oligo) represents uncoupled mitochondrial respiration, and carbonyl cyanide 4-(trifluoromethoxy) phenylhydrazone (FCCP) represents uncoupled mitochondrial respiration. **D**, Real-time quantitative polymerase chain reaction was used for the detection of *Anp* and *Myh7*. **E**, Scheme of the molecular mechanism of PRL2 dephosphorylation of AMPKα2. Data are shown as mean±SEM. N=3; **A**, **C**, and **D**, 1-way ANOVA followed by Tukey post hoc tests; *P* values indicated. AID indicates autoinhibitory sequence domain; CTD, carboxyl-terminal domain; EV, empty vector; and KD, kinase domain.

(Figure 8N; Figure S13B through S13D), suggesting that AMPKα2 is required for PLR2-mediated mitochondrial injury in mice. In addition, we noted that PRL2 knockdown did not affect cardiac physiology and function at the basal condition (Figure 8C through 8L; Figure S13A through S13D). Collectively, these results suggest that AMPKα2 mediates the cardioprotective effects of PRL2 deficiency in Ang II-challenged mice.

We also examined if AMPK activation mimics PRL2 deficiency in Ang II-infused mice using A769662, a direct allosteric activator of AMPK. Ang II-challenged WT and PRL2$^{-/-}$ mice were administered with A769662 (30 mg/kg) or vehicle for 2 weeks, respectively (Figure S14A). A769662 treatment did not affect the raised blood pressure in Ang II-infused PRL2$^{-/-}$ and WT mice (Figure S14B), while significantly reducing the serum concentration of ANP and the hypertrophic gene expression in hearts in Ang II-infused WT mice (Figure S14C through S14E). A769662 rescued the Ang II-induced cardiac dysfunction, hypertrophy, and fibrosis in WT mice (Figure S14F through S14P; Table S8). It is important to note that the cardioprotective effects of A769662 treatment are comparable to PRL2 deficiency in Ang II-infused mice, and A769662 failed to further protect hearts in Ang II-infused mice when PRL2 was deleted (Figure S14C through S14P; Table S8). Consistently, either A769662 or PRL2 knockout elevated the levels of p-AMPK, p-ACC, PPARα, PGC-1α, and mitochondrial

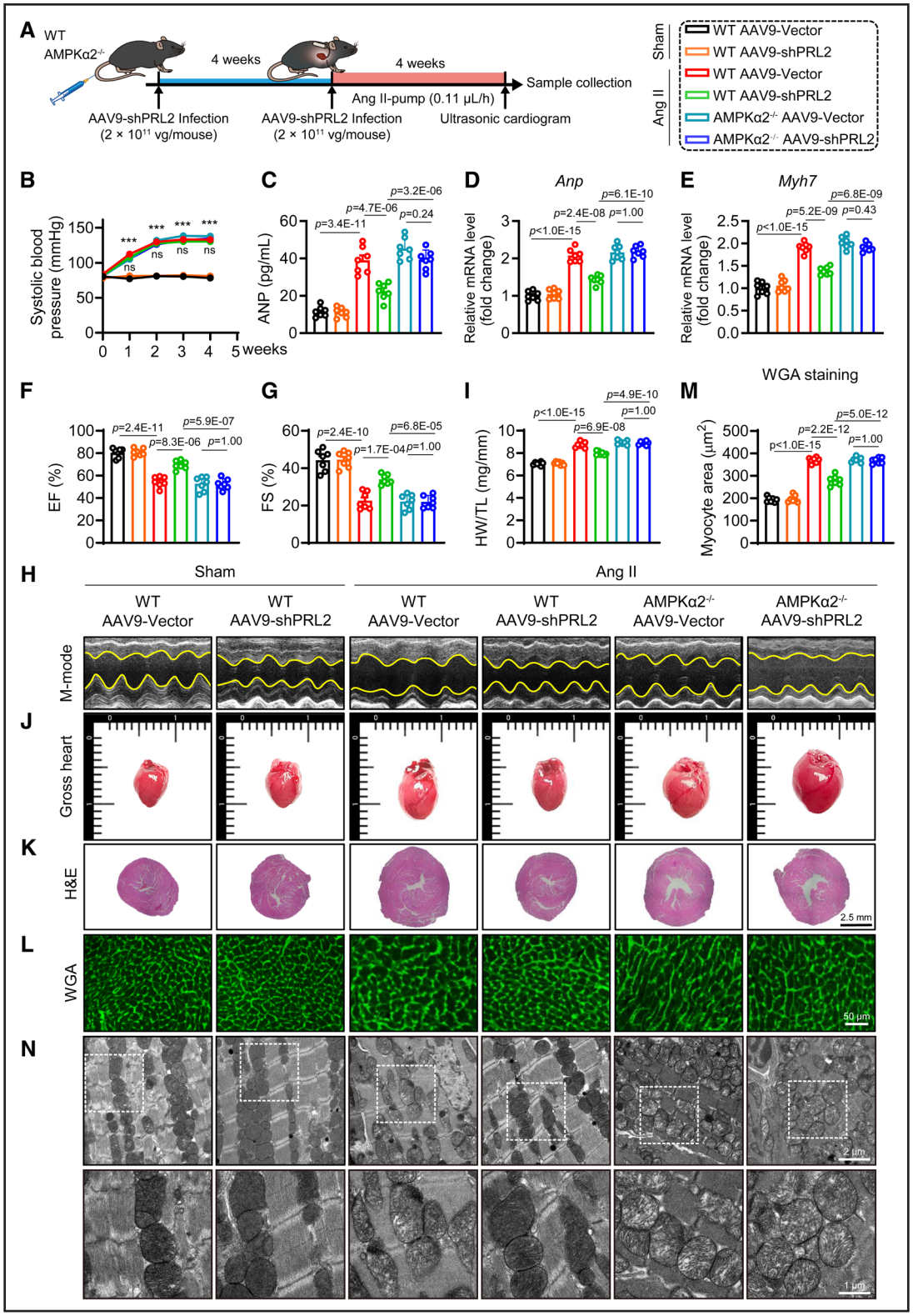

Figure 8. AMPKα2 (AMP-activated protein kinase) knockout abolished the protective effects of PRL2 (phosphatase of regenerative liver 2) deficiency against cardiac hypertrophy.

A, The adeno-associated virus 9 (AAV9)-shPRL2 or empty AAV9-Vector virus was injected into mice through the tail vein (2×10^{11} vg/mouse). Four weeks later, the mice were injected with the AAV9 virus again, followed by a 4-week infusion of angiotensin II (Ang II). **B**, The systolic blood pressure was detected in mice. ***$P<0.001$ vs Ang II-wild-type (WT) AAV9-vector; ns, no significance. **C**, Serum atrial natriuretic peptide (ANP) level was detected by the ELISA kit. **D** and **E**, Real-time quantitative polymerase chain reaction analysis of mRNA levels of *Anp* and *Myh7* in cardiac tissues. **F** and **G**, Values of ejection fraction (EF) and fractional shortening (FS). **H**, Representative M-mode echocardiographic images. **I**, The ratio of heart weight to tibia length ratios (HW/TL). **J**, Representative whole heart images. **K** through **M**, Representative (*Continued*)

score in the Ang II-challenged mouse heart tissues (Figure S14Q and S14R). These results further validate that AMPK activation is essential for PRL2 deficiency against cardiac hypertrophy in mice.

DISCUSSION

In this study, we found that PRL2 expression is upregulated in both human and mouse hypertrophic myocardium, especially in cardiomyocytes. Deletion of PRL2 mitigates cardiac dysfunction and hypertrophy in Ang II- or TAC-treated mouse models. Mechanistically, we provide the first evidence that PRL2 directly binds to the CTD of AMPKα2 and dephosphorylates AMPKα2 at the T172 site through its active site C46. Through regulating AMPK activity, PRL2 critically contributes to mitochondrial instability and FAO in Ang II-treated cardiomyocytes, resulting in hypertrophy and dysfunction in hearts. AMPKα2 knockout significantly diminishes the cardioprotective effects of PRL2 deficiency in Ang II-challenged mice. AMPK activation by A769662 mimics PRL2 deficiency against cardiac hypertrophy in Ang II-induced mice. This study provides PLR2 as a new target protein for future drug development treating HF. A schematic summary of the major findings is presented in the Graphical Abstract.

Protein dephosphorylation is a fundamental regulatory mechanism for protein posttranslational modification.[30] PTP family consists of 107 protein members. A previous study has found that the protein level of low molecular weight PTP is upregulated in mouse cardiac tissues under pressure overload, and gene deletion of low molecular weight PTP protects hearts against dysfunction and hypertrophy.[31] Conversely, deficiency of another PTP, PTP1B, shows deleterious effects on pathological hypertrophy.[32] In addition, scr homology-2 domain-bearing nontransmembrane PTP deficiency in cardiomyocytes could result in cardiomyopathy and premature death.[33] PRLs, a novel and relatively small subfamily in PTPs, have been reported to regulate the proliferation and migration of tumor cells.[20] Although PRL2 has been demonstrated to be involved in angiogenesis through regulating VEGF (vascular endothelial growth factor)-A and NOTCH-1 signaling in mouse retina,[23] no robust substrates for this subfamily have been reported to date. Through an RNA-sequencing analysis and a loss-of-function screen of PLR subfamily members, we identified PLR2 for the first time as an important regulator in pathological cardiac remodeling. The in vivo studies confirmed that PRL2 deficiency alleviated cardiac hypertrophy and dysfunction in mice upon Ang II or TAC challenge.

No explicit substrate for PRL2 phosphatase has been identified to date.[21] In this study, we identify that AMPK is a substrate of PRL2. Notably, PRL2-AMPK interaction is independent of Ang II induction. What Ang II does is induce PRL2 overexpression in cardiomyocytes, and then the increased PRL2 protein binds to more AMPK in heart tissues. As summarized by the previous review article, a series of downstream targets/pathways of AMPK have been reported to be responsible for preventing hypertrophy in cardiomyocytes, including regulating fatty acid synthesis, FAO, mitochondrial biogenesis, mitochondrial OXPHOS, and oxidative stress.[11,34] AMPK-mediated mitochondrial abnormality reduces cardiac ATP level and suppresses OXPHOS, which impairs systolic and diastolic function and induces pathological hypertrophy in cardiomyocyte.[10,11] In addition, dysfunctional mitochondria also increase intracellular reactive oxygen species production, which subsequently harms cardiomyocytes.[35] Inactivated AMPK and subsequent dysfunctions of mitochondria and fatty acid metabolism have been observed in TAC-induced cardiac hypertrophy mice.[36] This study reveals PRL2 as a novel AMPK-regulating phosphatase in cardiomyocytes. We examined some well-known downstream targets/pathways of AMPK activation, and our results supported that PRL2-mediated AMPK activation prevents cardiomyocyte hypertrophy and positively regulates these targets/pathways, including p-ACC, PPARα, PGC-1α, ATP content, mtDNA, mitochondrial respiratory, FAO, mitoSox, 8-OHdG, and 4-HNE levels. Therefore, we consider that PRL2-mediated AMPK activation prevents cardiomyocyte hypertrophy through the previously reported downstream targets/pathways.

Interestingly, it is still a little bit controversial if TAC increases or decreases AMPK activation in hypertrophic hearts. We summarized previous publications reporting AMPK activity in the TAC mouse model. Generally, TAC surgery seems to inactivate AMPK at the relatively short time points while inducing AMPK activation at relatively long time point.[10,25,37] In this study, we killed and examined the mice at 4 weeks after TAC. Previous studies agree with cardiac AMPK inactivation in response to TAC after 4 weeks.[10,25] Since the heart may be restored a long time after TAC surgery and the recovery of the heart needs AMPK activation-mediated energy metabolism, we may hypothesize that cardiac AMPK is inactivated during the pathological period after TAC (early stage), while AMPK activity is increased during the restorative period after TAC (later stage). In another word, AMPK inactivation should be pathological, and AMPK activation may be restorative in the hearts of mice with TAC. In addition, maintaining AMPK activation

Figure 8 Continued. images of hematoxylin and eosin (H&E) and wheat germ agglutinin (WGA) staining in heart samples, and quantitative analysis for WGA. **N**, Representative electron microscopic images of heart sections. Scale bar=2.5 m for H&E; 50 μm for WGA; 2 μm (**top**), and 1 μm (**bottom**) for electron microscopic images. Data are shown as mean±SEM. N=7; **B**, 2-way ANOVA followed by Tukey post hoc tests; **C**–**G**, **I**, and **M**, 1-way ANOVA followed by Tukey post hoc tests; *P* values indicated.

has been demonstrated as an effective strategy to preserve mitochondrial homeostasis and prevent cardiac hypertrophy, which also supports our finding. For example, AMPK activation improves mitochondrial function and decreases reactive oxygen species production and apoptosis of cardiomyocytes via phosphorylating PINK1, preventing the progression of cardiac hypertrophy.[10] Small-molecule AMPK activators, including metformin, 5-aminoimidazole-4-carboxamide ribonucleoside, and melatonin, have been reported to prevent cardiac hypertrophy via manipulating mitochondrial function in animal models.[38–40] Our study also confirmed the cardioprotective effects of the AMPK activator A769662.

Although some AMPK-activating compounds have been reported and tested, none of them have been approved for clinical use.[41] To date, no specifically designed AMPK activators have been applied in clinical trials.[42] It will be interesting to establish a more specific and safe manner to regulate AMPK activity in cardiomyocytes. Here, we found that PRL2 deficiency significantly attenuated Ang II-induced cardiac dysfunction through dephosphorylating AMPKα2, indicating that targeting PRL2 may be a new strategy to activate AMPK and then treat HF. From another perspective, designing and discovering an activator of a protein is much more difficult than the discovery of an inhibitor. It may be a more convenient strategy for medicinal chemists to design small-molecule PRL2 inhibitors with high druggability than to design small-molecule AMPK activators. Especially, we have demonstrated that PRL2 dephosphorylates T172 of AMPKα2 at T172 via its crucial active C46 site, and the CTD of AMPKα2 acted as a scaffold sustaining this posttranslational modification. Therefore, designing the small-molecule compounds, which can specifically block the protein-protein interaction between PRL2 and AMPKα2 CTD or specifically target the C46 residue in PRL2, may achieve an excellent selectivity and reduce the potential side effects. These findings provide important guidance for the design and discovery of specific PRL2 inhibitors treating HF.

Accumulating research has shown that the activity of AMPK is regulated by phosphorylating modification, and the ubiquitination of AMPK can influence and regulate its phosphorylation.[43,44] It has been reported that the active site T172 of AMPK could be phosphorylated by upstream kinases, such as LKB1 (liver kinase B1), TAK1 (TGF-β-activated kinase-1), and CaMKK (calcium-activated calmodulin-dependent kinase kinase).[44] AMPKα also could be ubiquitinating modification by ubiquitin-specific ligase USP10 or MG53, thereby promoting AMPKα phosphorylation by LKB1.[44,45] T172, S491, and S173 residues in AMPK have been reported to be phosphorylated by upstream kinases.[24] Among these 3 sites, T172 phosphorylation has been demonstrated to contribute mainly to the AMPK activity,[46,47] and dephosphorylating AMPK at T172 significantly inhibited AMPK and promoted mitochondrial injury in cardiomyocytes.[39,40,42] The present study, for the first time, illustrated the entire molecular process of PRL2-mediated AMPKα2^{T172} dephosphorylating modification in cardiomyocytes.

Structurally, the AMPK complex is composed of 1 catalytic α-subunit and 2 regulatory β- and γ-subunits.[48] The γ-subunit binds AMP, enabling AMPK phosphorylation of T172 in α2 subunit.[42] Based on the heterotrimeric complex of AMPK whose distribution depends on the species and tissue specificity,[49] the subunit-specific selectivity of AMPK may be beneficial to targeting specific tissues. In our experimental systems, PRL2 binds to AMPKα1 and α2 subunits, but not β1, β2, γ1, and γ2 subunits. The endogenous interaction experiment in NRPCs found that PRL2 predominantly bound to AMPKα2 but not α1, as the total AMPK α1 protein level in cardiomyocytes was low.[10] We also showed that the compensatory upregulation of AMPKα1 in AMPKα2$^{-/-}$ mice failed to change the whole situation of AMPK. The AMPKα2 subunit-specific regulation of PRL2 may afford the cardiac specificity of PRL2-targeting therapy. These results also suggest that it will be interesting to investigate the role of PRL2-AMPKα1 interaction in AMPKα1-containing cells (eg, hepatocytes) and AMPKα1-mediated diseases (eg, nonalcoholic fatty liver disease) in the future.

A limitation of this study may be that we did not use the cardiomyocyte-specific PRL2 knockout mice, while AAV9-mediated PRL2 knockdown specifically in cardiomyocytes validated the beneficial effects of cardiomyocyte PRL2 against cardiac hypertrophy in Ang II-challenged mice. In addition, we found that Ang II challenge time-dependently increased PRL2 protein in cardiomyocytes, whereas this phenomenon was not seen in fibroblasts, and PRL2 did not affect the pathological changes in Ang II-challenged myocardial microvascular endothelial cells. Another concerned question may be other substrates of PRL2 in cardiomyocytes. Although we selected AMPKα2 as the substrate of PRL2 via a strict screening and our in vivo data show that AMPKα2 knockout in cardiomyocytes significantly diminished the cardioprotective effects of PRL2 deficiency, it is difficult to completely exclude the potential involvement of other substrate proteins of PRL2.

In conclusion, we show that PRL2 directly binds to and then dephosphorylates AMPKα2 at the T172 site to promote mitochondrial dysfunction and pathological hypertrophy in cardiomyocytes. We reveal for the first time the protective effects of PRL2 deficiency against pathological cardiac hypertrophy in mice. These findings highlight an important role of PRL2 as an AMPK-regulating PTP in cardiac pathology, suggesting that future pharmacological inhibition or gene therapy targeting PRL2 may represent a promising therapeutic strategy for HF.

ARTICLE INFORMATION

Received July 17, 2024; revision received January 18, 2025; accepted January 31, 2025.

Affiliations

Department of Pharmacy and Institute of Inflammation, Zhejiang Provincial People's Hospital, Affiliated People's Hospital (X.H., Y.Z., Y.W., G.L.), Zhejiang Provincial Key Laboratory of Laboratory Animals and Safety Research (X.H., Q.S., Y.T., J.Z., W.L., Y.L., R.Z., J.W., H.Y.), and School of Pharmaceutical Sciences (S.Y., Y.Z., G.L.), Hangzhou Medical College, Zhejiang, China. Department of Pharmacology, College of Pharmacy, Beihua University, Jilin, China (M.W.). Department of Cardiology, the First Affiliated Hospital of Wenzhou Medical University, Zhejiang, China (X.H., S.Y., B.Y., G.L.).

Author Contrinbutions

G. Liang, H. Ying, and X. Han contributed to the literature search and study design. G. Liang, X. Han, Q. Shi, and Y. Wang participated in the drafting of the article. X. Han, Q. Shi, Y. Tu, J. Zhang, M. Wang, W. Li, Y. Liu, R. Zheng, J. Wei, and Y. Zhang performed the experiments. S. Ye and B. Ye collected the clinical samples. G. Liang, H. Ying, X. Han, and Q. Shi revised the manuscript. X. Han and Y. Tu contributed to data collection and analysis.

Sources of Funding

This study was supported by the National Natural Science Foundation of China (grant nos. 81930108 to G. Liang and 82370244 to Y. Wang), the Natural Science Foundation of Zhejiang Province (grant no. LTGD24C040007 to Q. Shi), and the Medical Scientific Research Foundation of Zhejiang Province (grant no. 2024KY932 to X. Han).

Disclosures

None.

Supplemental Material

Expanded Materials and Methods
Figures S1-S14
Tables S1-S9
References 3,26,27,50–53

REFERENCES

1. Ritterhoff J, Tian R. Metabolic mechanisms in physiological and pathological cardiac hypertrophy: new paradigms and challenges. *Nat Rev Cardiol*. 2023;20:812–829. doi: 10.1038/s41569-023-00887-x
2. Ye S, Huang H, Han X, Luo W, Wu L, Ye Y, Gong Y, Zhao X, Huang W, Wang Y, et al. Dectin-1 acts as a non-classical receptor of Ang II to induce cardiac remodeling. *Circ Res*. 2023;132:707–722. doi: 10.1161/CIRCRESAHA.122.322259
3. Ye B, Zhou H, Chen Y, Luo W, Lin W, Zhao Y, Han J, Han X, Huang W, Wu G, et al. USP25 ameliorates pathological cardiac hypertrophy by stabilizing SERCA2a in cardiomyocytes. *Circ Res*. 2023;132:465–480. doi: 10.1161/CIRCRESAHA.122.321849
4. Zhuang L, Jia K, Chen C, Li Z, Zhao J, Hu J, Zhang H, Fan Q, Huang C, Xie H, et al. DYRK1B-STAT3 drives cardiac hypertrophy and heart failure by impairing mitochondrial bioenergetics. *Circulation*. 2022;145:829–846. doi: 10.1161/CIRCULATIONAHA.121.055727
5. Da Dalt L, Cabodevilla AG, Goldberg IJ, Norata GD. Cardiac lipid metabolism, mitochondrial function, and heart failure. *Cardiovasc Res*. 2023;119:1905–1914. doi: 10.1093/cvr/cvad100
6. Lin HB, Naito K, Oh Y, Farber G, Kanaan G, Valaperti A, Dawood F, Zhang L, Li GH, Smyth D, et al. Innate immune Nod1/RIP2 signaling is essential for cardiac hypertrophy but requires mitochondrial antiviral signaling protein for signal transductions and energy balance. *Circulation*. 2020;142:2240–2258. doi: 10.1161/CIRCULATIONAHA.119.041213
7. Teixeira RB, Pfeiffer M, Zhang P, Shafique E, Rayta B, Karbasiafshar C, Ahsan N, Sellke FW, Abid MR. Reduction in mitochondrial ROS improves oxidative phosphorylation and provides resilience to coronary endothelium in non-reperfused myocardial infarction. *Basic Res Cardiol*. 2023;118:3. doi: 10.1007/s00395-022-00976-x
8. Kumar AA, Kelly DP, Chirinos JA. Mitochondrial dysfunction in heart failure with preserved ejection fraction. *Circulation*. 2019;139:1435–1450. doi: 10.1161/CIRCULATIONAHA.118.036259
9. Jin L, Geng L, Ying L, Shu L, Ye K, Yang R, Liu Y, Wang Y, Cai Y, Jiang X, et al. FGF21-Sirtuin 3 axis confers the protective effects of exercise against diabetic cardiomyopathy by governing mitochondrial integrity. *Circulation*. 2022;146:1537–1557. doi: 10.1161/CIRCULATIONAHA.122.059631
10. Wang B, Nie J, Wu L, Hu Y, Wen Z, Dong L, Zou MH, Chen C, Wang DW. AMPKalpha2 protects against the development of heart failure by enhancing mitophagy via PINK1 phosphorylation. *Circ Res*. 2018;122:712–729. doi: 10.1161/CIRCRESAHA.117.312317
11. Zaha V, Young L. AMP-activated protein kinase regulation and biological actions in the heart. *Circ Res*. 2012;111:800–814. doi: 10.1161/CIRCRESAHA.111.255505
12. Sakaguchi T, Takefuji M, Wettschureck N, Hamaguchi T, Amano M, Kato K, Tsuda T, Eguchi S, Ishihama S, Mori Y, et al. Protein kinase N promotes stress-induced cardiac dysfunction through phosphorylation of Myocardin-related transcription factor A and disruption of its interaction with actin. *Circulation*. 2019;140:1737–1752. doi: 10.1161/CIRCULATIONAHA.119.041019
13. Kim M, Morales LD, Jang IS, Cho YY, Kim DJ. Protein tyrosine phosphatases as potential regulators of STAT3 signaling. *Int J Mol Sci* . 2018;19:2708. doi:10.3390/ijms19092708
14. Sharma C, Kim Y, Ahn D, Chung SJ. Protein tyrosine phosphatases (PTPs) in diabetes: causes and therapeutic opportunities. *Arch Pharm Res*. 2021;44:310–321. doi: 10.1007/s12272-021-01315-9
15. Crunkhorn S. Metabolic disease: protein tyrosine phosphatase inhibitor reverses diabetes. *Nat Rev Drug Discov*. 2017;16:312–313. doi: 10.1038/nrd.2017.73
16. Ohtake Y, Saito A, Li S. Diverse functions of protein tyrosine phosphatase sigma in the nervous and immune systems. *Exp Neurol*. 2018;302:196–204. doi: 10.1016/j.expneurol.2018.01.014
17. Scott LM, Chen L, Daniel KG, Brooks WH, Guida WC, Lawrence HR, Sebti SM, Lawrence NJ, Wu J. Shp2 protein tyrosine phosphatase inhibitor activity of estramustine phosphate and its triterpenoid analogs. *Bioorg Med Chem Lett*. 2011;21:730–733. doi: 10.1016/j.bmcl.2010.11.117
18. Scott LM, Lawrence HR, Sebti SM, Lawrence NJ, Wu J. Targeting protein tyrosine phosphatases for anticancer drug discovery. *Curr Pharm Des*. 2010;16:1843–1862. doi: 10.2174/138161210791209027
19. Wade F, Belhaj K, Poizat C. Protein tyrosine phosphatases in cardiac physiology and pathophysiology. *Heart Fail Rev*. 2018;23:261–272. doi: 10.1007/s10741-018-9676-1
20. Wei M, Korotkov KV, Blackburn JS. Targeting phosphatases of regenerating liver (PRLs) in cancer. *Pharmacol Ther*. 2018;190:128–138. doi: 10.1016/j.pharmthera.2018.05.014
21. Hardy S, Kostantin E, Hatzihristidis T, Zolotarov Y, Uetani N, Tremblay ML. Physiological and oncogenic roles of the PRL phosphatases. *FEBS J*. 2018;285:3886–3908. doi: 10.1111/febs.14503
22. Dong YS, Zhang LJ, Zhang S, Bai YP, Chen HY, Sun XX, Yong WD, Li W, Colvin SC, Rhodes SJ, et al. Phosphatase of regenerating liver 2 (PRL2) is essential for placental development by down-regulating PTEN (Phosphatase and Tensin Homologue Deleted on Chromosome 10) and activating Akt protein. *J Biol Chem*. 2012;287:32172–32179. doi: 10.1074/jbc.m112.393462
23. Poulet M, Sirois J, Boye K, Uetani N, Hardy S, Daubon T, Dubrac A, Tremblay ML, Bikfalvi A. PRL-2 phosphatase is required for vascular morphogenesis and angiogenic signaling. *Commun Biol*. 2020;3:603. doi: 10.1038/s42003-020-01343-z
24. Hornbeck PV, Zhang B, Murray B, Kornhauser JM, Latham V, Skrzypek E. PhosphoSitePlus, 2014: mutations, PTMs and recalibrations. *Nucleic Acids Res*. 2015;43:D512–D520. doi: 10.1093/nar/gku1267
25. Zhang X, Zhang Z, Wang P, Han Y, Liu L, Li J, Chen Y, Liu D, Wang J, Tian X, et al. Bawei Chenxiang Wan ameliorates cardiac hypertrophy by activating AMPK/PPAR-α signaling pathway improving energy metabolism. *Front Pharmacol*. 2021;12:653901. doi: 10.3389/fphar.2021.653901
26. Yamamoto T, Maurya S, Pruzinsky E, Batmanov K, Xiao Y, Sulon S, Sakamoto T, Wang Y, Lai L, McDaid K, et al. RIP140 deficiency enhances cardiac fuel metabolism and protects mice from heart failure. *J Clin Invest*. 2023;133:e162309. doi: 10.1172/JCI162309
27. Hsieh CC, Li CY, Hsu CH, Chen HL, Chen YH, Liu YP, Liu YR, Kuo HF, Liu PL. Mitochondrial protection by simvastatin against angiotensin II-mediated heart failure. *Br J Pharmacol*. 2019;176:3791–3804. doi: 10.1111/bph.14781
28. Saito T, Uchiumi T, Yagi M, Amamoto R, Setoyama D, Matsushima Y, Kang D. Cardiomyocyte-specific loss of mitochondrial p32/C1qbp causes cardiomyopathy and activates stress responses. *Cardiovasc Res*. 2017;113:1173–1185. doi: 10.1093/cvr/cvx095
29. Li Z, Hu O, Xu S, Lin C, Yu W, Ma D, Lu J, Liu P. The SIRT3-ATAD3A axis regulates MAM dynamics and mitochondrial calcium homeostasis in cardiac hypertrophy. *Int J Biol Sci*. 2024;20:831–847. doi: 10.7150/ijbs.89253

30. Abdollahi P, Kohn M, Borset M. Protein tyrosine phosphatases in multiple myeloma. *Cancer Lett.* 2021;501:105–113. doi: 10.1016/j.canlet.2020.11.042
31. Wade F, Quijada P, Al-Haffar KM, Awad SM, Kunhi M, Toko H, Marashly Q, Belhaj K, Zahid I, Al-Mohanna F, et al. Deletion of low molecular weight protein tyrosine phosphatase (Acp1) protects against stress-induced cardiomyopathy. *J Pathol.* 2015;237:482–494. doi: 10.1002/path.4594
32. Coulis G, Londhe AD, Sagabala RS, Shi Y, Labbé DP, Bergeron A, Sahadevan P, Nawaito SA, Sahmi F, Josse M, et al. Protein tyrosine phosphatase 1B regulates miR-208b Argonaute 2 association and thyroid hormone responsiveness in cardiac hypertrophy. *Sci Signal.* 2022;15:eabn6875. doi: 10.1126/scisignal.abn6875
33. Princen F, Bard E, Sheikh F, Zhang SS, Wang J, Zago WM, Wu D, Trelles RD, Bailly-Maitre B, Kahn CR, et al. Deletion of Shp2 tyrosine phosphatase in muscle leads to dilated cardiomyopathy, insulin resistance, and premature death. *Mol Cell Biol.* 2009;29:378–388. doi: 10.1128/MCB.01661-08
34. Rosca MG, Tandler B, Hoppel CL. Mitochondria in cardiac hypertrophy and heart failure. *J Mol Cell Cardiol.* 2013;55:31–41. doi: 10.1016/j.yjmcc.2012.09.002
35. Zheng H, Huang S, Wei G, Sun Y, Li L, Si X, Chen Y, Tang Z, Li X, Chen Y, et al. CircRNA Samd4 induces cardiac repair after myocardial infarction by blocking mitochondria-derived ROS output. *Mol Ther.* 2022;30:3477–3498. doi: 10.1016/j.ymthe.2022.06.016
36. Xu M, Xue RQ, Lu Y, Yong SY, Wu Q, Cui YL, Zuo XT, Yu XJ, Zhao M, Zang WJ. Choline ameliorates cardiac hypertrophy by regulating metabolic remodelling and UPRmt through SIRT3-AMPK pathway. *Cardiovasc Res.* 2019;115:530–545. doi: 10.1093/cvr/cvy217
37. Tian R, Musi N, D'Agostino J, Hirshman M, Goodyear L. Increased adenosine monophosphate-activated protein kinase activity in rat hearts with pressure-overload hypertrophy. *Circulation.* 2001;104:1664–1669. doi: 10.1161/hc4001.097183
38. Salvatore T, Galiero R, Caturano A, Vetrano E, Rinaldi L, Coviello F, Di Martino A, Albanese G, Marfella R, Sardu C, et al. Effects of metformin in heart failure: from pathophysiological rationale to clinical evidence. *Biomolecules.* 2021;11:1834. doi: 10.3390/biom11121834
39. Zhang Y, Mi SL, Hu N, Doser TA, Sun A, Ge J, Ren J. Mitochondrial aldehyde dehydrogenase 2 accentuates aging-induced cardiac remodeling and contractile dysfunction: role of AMPK, Sirt1, and mitochondrial function. *Free Radic Biol Med.* 2014;71:208–220. doi: 10.1016/j.freeradbiomed.2014.03.018
40. Zhang Y, Wang Y, Xu J, Tian F, Hu S, Chen Y, Fu Z. Melatonin attenuates myocardial ischemia-reperfusion injury via improving mitochondrial fusion/mitophagy and activating the AMPK-OPA1 signaling pathways. *J Pineal Res.* 2019;66:e12542. doi: 10.1111/jpi.12542
41. Steinberg GR, Carling D. AMP-activated protein kinase: the current landscape for drug development. *Nat Rev Drug Discov.* 2019;18:527–551. doi: 10.1038/s41573-019-0019-2
42. Sharma A, Anand SK, Singh N, Dwivedi UN, Kakkar P. AMP-activated protein kinase: An energy sensor and survival mechanism in the reinstatement of metabolic homeostasis. *Exp Cell Res.* 2023;428:113614. doi: 10.1016/j.yexcr.2023.113614
43. Jin L, Chun J, Pan C, Kumar A, Zhang G, Ha Y, Li D, Alesi GN, Kang Y, Zhou L, et al. The PLAG1-GDH1 axis promotes Anoikis resistance and tumor metastasis through CamKK2-AMPK signaling in LKB1-Deficient lung cancer. *Mol Cell.* 2018;69:87–99.e7. doi: 10.1016/j.molcel.2017.11.025
44. Deng M, Yang X, Qin B, Liu T, Zhang H, Guo W, Lee SB, Kim JJ, Yuan J, Pei H, et al. Deubiquitination and activation of AMPK by USP10. *Mol Cell.* 2016;61:614–624. doi: 10.1016/j.molcel.2016.01.010
45. Jiang P, Ren L, Zhi L, Yu Z, Lv F, Xu F, Peng W, Bai X, Cheng K, Quan K, et al. Negative regulation of AMPK signaling by high glucose via E3 ubiquitin ligase MG53. *Mol Cell.* 2021;81:629–637.e5. doi: 10.1016/j.molcel.2020.12.008
46. Tang X, Chen XF, Wang NY, Wang XM, Liang ST, Zheng W, Lu YB, Zhao X, Hao DL, Zhang ZQ, et al. SIRT2 acts as a Cardioprotective deacetylase in pathological cardiac hypertrophy. *Circulation.* 2017;136:2051–2067. doi: 10.1161/CIRCULATIONAHA.117.028728
47. Shaw RJ, Kosmatka M, Kosmatka N, Hurley RL, Witters LA, DePinho RA, Cantley LC. The tumor suppressor LKB1 kinase directly activates AMP-activated kinase and regulates apoptosis in response to energy stress. *Proc Natl Acad Sci USA.* 2004;101:3329–3335. doi: 10.1073/pnas.0308061100
48. Herzig S, Shaw RJ. AMPK: guardian of metabolism and mitochondrial homeostasis. *Nat Rev Mol Cell Biol.* 2018;19:121–135. doi: 10.1038/nrm.2017.95
49. Madhavi YV, Gaikwad N, Yerra VG, Kalvala AK, Nanduri S, Kumar A. Targeting AMPK in diabetes and diabetic complications: energy homeostasis, autophagy and mitochondrial health. *Curr Med Chem.* 2019;26:5207–5229. doi: 10.2174/0929867325666180406120051
50. Medzikovic L, Aryan L, Eghbali M. Connecting sex differences, estrogen signaling, and microRNAs in cardiac fibrosis. *J Mol Med (Berl).* 2019;97:1385–1398. doi: 10.1007/s00109-019-01833-6
51. Ye S, Luo W, Khan ZA, Wu G, Xuan L, Shan P, Lin K, Chen T, Wang J, Hu X, et al. Celastrol attenuates angiotensin II-induced cardiac remodeling by targeting STAT3. *Circ Res.* 2020;126:1007–1023. doi: 10.1161/CIRCRESAHA.119.315861
52. Townsend L, Weber A, Day E, Shamshoum H, Shaw S, Perry C, Kemp B, Steinberg G, Wright D. AMPK mediates energetic stress-induced liver GDF15. *FASEB J.* 2021;35:e21218. doi: 10.1096/fj.202000954R
53. Zhao Q, Luo T, Gao F, Fu Y, Li B, Shao X, Chen H, Zhou Z, Guo S, Shen L, et al. GRP75 regulates mitochondrial-Supercomplex turnover to modulate insulin sensitivity. *Diabetes.* 2022;71:233–248. doi: 10.2337/db21-0173